With regard to our initial GWAS conducted as a consecutive three-stage analysis, the lowest combined *P*-value for the entire sample was $P = 8.044 \times 10^{-7}$ (Supplementary Table S2), which would have been deemed genome-wide nonsignificant if only a single-stage analysis was used to calculate conventional Bonferroni- or false discovery rate-corrected *P*-values for the total samples to determine statistical significance. However, 'significant' results obtained as conventionally corrected *P*-values will not always represent true associations, meaning that the results may not be necessarily replicated in other studies, and vice versa. For example, data from the National Human Genome Research Institute GWAS catalog (as of 31 January 2009), show 1321 entries of discovered associations with a *P*-value of $<10^{-5}$, but only 550 of these entries have a *P*-value of $<5 \times 10^{-8}$,[44] which is a conventionally corrected conservative threshold for declaring a significant association in a GWAS.[45,46] In both cases, truly potent candidate SNPs may be included in the outcome of the studies. Furthermore, GWASs in pharmacogenomics, such as this study, would tend not to yield 'significant' results obtained as conventionally corrected *P*-values compared with complex-disease GWASs[15] for several reasons. Among at least 16 different GWASs on drug response since the first was published in late 2007, less than half have shown genome-wide significance, although some potentially interesting associations that come close to significance have been detected in several of the studies in this category.[15] Altogether, these reports suggest that conventionally corrected *P*-values for the combined samples are not the only criteria to find true associations between SNPs and the phenotypes examined. The SNP we found, rs2952768, appears to be a promising SNP that is associated not only with opioid analgesic sensitivity in two independent surgical operations but also with several dependence-related traits in other subjects, prompting us to consider this SNP as the best candidate SNP known to date that is truly associated with human opioid sensitivity.

Our compelling results suggest the possibility that the association observed in this study can be robustly generalized to various clinical and nonclinical scenarios, although this study is rather exploratory, and independent confirmation of the findings will be required in subsequent studies before various forms of practical clinical utilization of the prediction of opioid sensitivity based on this SNP can be applied. In conclusion, although the underlying mechanisms remain to be fully elucidated in future studies, our findings provide a novel step toward understanding individual differences in opioid sensitivity and stimulating future studies that can open new avenues for the personalized treatment of pain and drug dependence.

CONFLICT OF INTEREST

The authors declare no conflict of interest.

ACKNOWLEDGEMENTS

We acknowledge Dr Keiji Tanaka for critically reading the manuscript and Mr Michael Arends for his assistance with editing the manuscript. We are grateful to the volunteers for their participation in this study and the anesthesiologists, surgeons and psychiatrists at related hospitals for collecting clinical data. We thank the Stanley Medical Research Institute Brain Collection for donating specimens. This work was supported by grants from the MEXT of Japan (20390162, 23390377), MHLW of Japan (H21-3jigan-ippan-011, H22-Iyaku -015) and Smoking Research Foundation.

AUTHOR CONTRIBUTIONS

Conception and design of the experiments: DN, SK and KI. Performance of the experiments: DN, SK, JH and AN. Analysis of the data: DN and YA Contribution of reagents/materials/analysis tools: DN, JH, AN, MK and TA. Writing of the paper: DN and KI. Collection of clinical data and DNA: KF, NS, Y Koukita, MN, RK, YS, MT, SH, HU, NO, TI, NI, IS, M Iyo, NK, MW, NN, KU, M Itokawa and MH. Support of the collection of clinical data and DNA: Y Kaneko.

REFERENCES

1 Sora I, Takahashi N, Funada M, Ujike H, Revay RS, Donovan DM *et al.* Opiate receptor knockout mice define mu receptor roles in endogenous nociceptive responses and morphine-induced analgesia. *Proc Natl Acad Sci USA* 1997; **94**: 1544–1549.
2 Leknes S, Tracey I. A common neurobiology for pain and pleasure. *Nat Rev Neurosci* 2008; **9**: 314–320.
3 Sora I, Elmer G, Funada M, Pieper J, Li XF, Hall FS *et al.* μ Opiate receptor gene dose effects on different morphine actions: evidence for differential in vivo mu receptor reserve. *Neuropsychopharmacology* 2001; **25**: 41–54.
4 Hall FS, Sora I, Uhl GR. Ethanol consumption and reward are decreased in μ-opiate receptor knockout mice. *Psychopharmacology (Berl)* 2001; **154**: 43–49.
5 Hall FS, Goeb M, Li XF, Sora I, Uhl GR. μ-Opioid receptor knockout mice display reduced cocaine conditioned place preference but enhanced sensitization of cocaine-induced locomotion. *Brain Res Mol Brain Res* 2004; **121**: 123–130.
6 Contarino A, Picetti R, Matthes HW, Koob GF, Kieffer BL, Gold LH. Lack of reward and locomotor stimulation induced by heroin in mu-opioid receptor-deficient mice. *Eur J Pharmacol* 2002; **446**: 103–109.
7 Berrendero F, Kieffer BL, Maldonado R. Attenuation of nicotine-induced antinociception, rewarding effects, and dependence in mu-opioid receptor knock-out mice. *J Neurosci* 2002; **22**: 10935–10940.
8 Shen X, Purser C, Tien LT, Chiu CT, Paul IA, Baker R *et al.* μ-Opioid receptor knockout mice are insensitive to methamphetamine-induced behavioral sensitization. *J Neurosci Res* 2010; **88**: 2294–2302.
9 Ikeda K, Ide S, Han W, Hayashida M, Uhl GR, Sora I. How individual sensitivity to opiates can be predicted by gene analyses. *Trends Pharmacol Sci* 2005; **26**: 311–317.
10 Coulbault L, Beaussier M, Verstuyft C, Weickmans H, Dubert L, Tregouet D *et al.* Environmental and genetic factors associated with morphine response in the postoperative period. *Clin Pharmacol Ther* 2006; **79**: 316–324.
11 Nishizawa D, Nagashima M, Katoh R, Satoh Y, Tagami M, Kasai S *et al.* Association between *KCNJ6* (*GIRK2*) gene polymorphisms and postoperative analgesic requirements after major abdominal surgery. *PLoS One* 2009; **4**: e7060.
12 Fukuda K, Hayashida M, Ide S, Saita N, Kokita Y, Kasai S *et al.* Association between *OPRM1* gene polymorphisms and fentanyl sensitivity in patients undergoing painful cosmetic surgery. *Pain* 2009; **147**: 194–201.
13 Candiotti KA, Yang Z, Morris R, Yang J, Crescimone NA, Sanchez GC *et al.* Polymorphism in the interleukin-1 receptor antagonist gene is associated with serum interleukin-1 receptor antagonist concentrations and postoperative opioid consumption. *Anesthesiology* 2011; **114**: 1162–1168.
14 Kumar D, Deb I, Chakraborty J, Mukhopadhyay S, Das S. A polymorphism of the CREB binding protein (CREBBP) gene is a risk factor for addiction. *Brain Res* 2011; **1406**: 59–64.
15 Daly AK. Genome-wide association studies in pharmacogenomics. *Nat Rev Genet* 2010; **11**: 241–246.
16 Wang L, McLeod HL, Weinshilboum RM. Genomics and drug response. *N Engl J Med* 2011; **364**: 1144–1153.
17 Feero WG, Guttmacher AE, Collins FS. Genomic medicine—an updated primer. *N Engl J Med* 2010; **362**: 2001–2011.
18 Hayashida M, Nagashima M, Satoh Y, Katoh R, Tagami M, Ide S *et al.* Analgesic requirements after major abdominal surgery are associated with *OPRM1* gene polymorphism genotype and haplotype. *Pharmacogenomics* 2008; **9**: 1605–1616.
19 Cloninger CR. A systematic method for clinical description and classification of personality variants. A proposal. *Arch Gen Psychiatry* 1987; **44**: 573–588.
20 Cloninger CR, Svrakic DM, Przybeck TR. A psychobiological model of temperament and character. *Arch Gen Psychiatry* 1993; **50**: 975–990.
21 Svrakic DM, Whitehead C, Przybeck TR, Cloninger CR. Differential diagnosis of personality disorders by the seven-factor model of temperament and character. *Arch Gen Psychiatry* 1993; **50**: 991–999.
22 Ujike H, Harano M, Inada T, Yamada M, Komiyama T, Sekine Y *et al.* Nine- or fewer repeat alleles in VNTR polymorphism of the dopamine transporter gene is a strong risk factor for prolonged methamphetamine psychosis. *Pharmacogenomics J* 2003; **3**: 242–247.
23 Ujike H. [Japanese Genetics Initiative for Drug Abuse (JGIDA)]. *Nihon Shinkei Seishin Yakurigaku Zasshi = Japanese Journal of Psychopharmacology* 2004; **24**: 299–302.
24 Benjamini Y, Hochberg Y. Controlling the false discovery rate: a practical and powerful approach to multiple testing. *J R Statist Soc B.* 1995; **57**: 289–300.
25 Storey J. The positive false discovery rate: a Bayesian interpretation and the q-value. *Ann Statist* 2001; **31**: 2013–2035.
26 Purcell S, Neale B, Todd-Brown K, Thomas L, Ferreira MA, Bender D *et al.* PLINK: a tool set for whole-genome association and population-based linkage analyses. *Am J Hum Genet* 2007; **81**: 559–575.

27 Barrett JC, Fry B, Maller J, Daly MJ. Haploview: analysis and visualization of LD and haplotype maps. *Bioinformatics* 2005; **21**: 263–265.
28 Nyholt DR. Genetic case-control association studies—correcting for multiple testing. *Hum Genet* 2001; **109**: 564–567.
29 Perneger TV. What's wrong with Bonferroni adjustments. *BMJ* 1998; **316**: 1236–1238.
30 Hakamata Y, Iwase M, Iwata H, Kobayashi T, Tamaki T, Nishio M *et al.* Regional brain cerebral glucose metabolism and temperament: a positron emission tomography study. *Neurosci Lett* 2006; **396**: 33–37.
31 Zink CF, Pagnoni G, Martin-Skurski ME, Chappelow JC, Berns GS. Human striatal responses to monetary reward depend on saliency. *Neuron* 2004; **42**: 509–517.
32 Law PY, Wong YH, Loh HH. Molecular mechanisms and regulation of opioid receptor signaling. *Annu Rev Pharmacol Toxicol* 2000; **40**: 389–430.
33 Childers SR. Opioid receptors: pinning down the opiate targets. *Curr Biol* 1997; **7**: R695–R697.
34 Ikeda K, Kobayashi T, Kumanishi T, Yano R, Sora I, Niki H. Molecular mechanisms of analgesia induced by opioids and ethanol: is the GIRK channel one of the keys? *Neurosci Res* 2002; **44**: 121–131.
35 Carlezon Jr WA, Thome J, Olson VG, Lane-Ladd SB, Brodkin ES, Hiroi N *et al.* Regulation of cocaine reward by CREB. *Science* 1998; **282**: 2272–2275.
36 Nestler EJ. Molecular mechanisms of drug addiction. *Neuropharmacology* 2004; **47**(Suppl 1): 24–32.
37 Ho IK, Loh HH, Way EL. Cyclic adenosine monophosphate antagonism of morphine analgesia. *J Pharmacol Exp Ther* 1973; **185**: 336–346.
38 Kim KS, Lee KW, Im JY, Yoo JY, Kim SW, Lee JK *et al.* Adenylyl cyclase type 5 (AC5) is an essential mediator of morphine action. *Proc Natl Acad Sci USA* 2006; **103**: 3908–3913.
39 Barrot M, Olivier JD, Perrotti LI, DiLeone RJ, Berton O, Eisch AJ *et al.* CREB activity in the nucleus accumbens shell controls gating of behavioral responses to emotional stimuli. *Proc Natl Acad Sci USA* 2002; **99**: 11435–11440.
40 Maldonado R, Blendy JA, Tzavara E, Gass P, Roques BP, Hanoune J *et al.* Reduction of morphine abstinence in mice with a mutation in the gene encoding CREB. *Science* 1996; **273**: 657–659.
41 Walters CL, Godfrey M, Li X, Blendy JA. Alterations in morphine-induced reward, locomotor activity, and thermoregulation in CREB-deficient mice. *Brain Res* 2005; **1032**: 193–199.
42 Richon VM, Johnston D, Sneeringer CJ, Jin L, Majer CR, Elliston K *et al.* Chemogenetic analysis of human protein methyltransferases. *Chem Biol Drug Des* 2011; **78**: 199–210.
43 Wang J, Barke RA, Roy S. Transcriptional and epigenetic regulation of interleukin-2 gene in activated T cells by morphine. *J Biol Chem* 2007; **282**: 7164–7171.
44 Ioannidis JP, Thomas G, Daly MJ. Validating, augmenting and refining genome-wide association signals. *Nat Rev Genet* 2009; **10**: 318–329.
45 Hirschhorn JN, Daly MJ. Genome-wide association studies for common diseases and complex traits. *Nat Rev Genet* 2005; **6**: 95–108.
46 Risch N, Merikangas K. The future of genetic studies of complex human diseases. *Science* 1996; **273**: 1516–1517.

Supplementary Information accompanies the paper on the Molecular Psychiatry website (http://www.nature.com/mp)

Schizophrenia Research 137 (2012) 264–266

Contents lists available at SciVerse ScienceDirect

Schizophrenia Research

journal homepage: www.elsevier.com/locate/schres

Letter to the Editor

A two-stage case–control association study between the tryptophan hydroxylase 2 (*TPH2*) gene and schizophrenia in a Japanese population

Dear Editors,

Serotonin has been shown to be involved in neurobiological mechanisms underlying schizophrenia (Abi-Dargham, 2007). The gene encoding tryptophan hydroxylase 2 (TPH2), the rate-limiting enzyme in brain serotonin synthesis (Walther et al., 2003), could serve as a candidate gene for schizophrenia. Previous studies have failed to provide evidence for an association between *TPH2* and schizophrenia (De Luca et al., 2005; Higashi et al., 2007; Shiroiwa et al., 2010; Tee et al., 2010; Kim and Yoon, 2011; Serretti et al., 2011; Zhang et al., 2011). However, these studies were performed with relatively small sample sizes and a limited number of markers. A two-stage case–control association study in Japanese individuals was performed to assess whether *TPH2* is implicated in schizophrenia vulnerability.

The present study was approved by the Ethics Committee of each participating institute, and written informed consent was obtained from all participants. The screening population comprised 626 patients with schizophrenia (333 men and 293 women; mean age 39.9 ± 13.9 years) and 620 mentally healthy individuals (317 men and 303 women; mean age 38.2 ± 10.6 years). Controls were identical to our previous association study of *TPH2* with autism spectrum disorders (Egawa et al., 2011). The confirmatory population comprised 2007 patients (1079 men and 928 women; mean age 47.2 ± 14.3 years) and 2195 controls (1165 men and 1030 women; mean age 46.6 ± 13.8 years). Psychiatric assessment was conducted in each participant as previously described (Watanabe et al., 2006).

A total of 17 tagging single nucleotide polymorphisms (SNPs) for *TPH2* (chr12:70617063.70712616) were selected from the HapMap database (http://hapmap.ncbi.nlm.nih.gov/) as previously described (Watanabe et al., 2010a). However, a TaqMan probe for rs1179001 was not designed and, therefore, the SNP was excluded.

The *TPH2* coding regions (RefSeq accession number, NG_008279.1) were resequenced in 101 patients who were included in the screening population using direct sequencing of PCR products (Supplementary Table 1) as previously described (Nunokawa et al., 2010). Of seven sequence variations detected (Supplementary Table 2), a missense variation was rs78162420 (p.S41Y). In addition, we also included rs139896303 (p.R225Q) which was detected in a patient with autistic disorder in our previous study (Egawa et al., 2011).

All SNPs were genotyped using the TaqMan 5′-exonuclease assay (Applied Biosystems, Foster City, CA; Supplementary Table 3) as previously described (Watanabe et al., 2006).

We investigated two common intronic copy number variations (CNVs) of *TPH2*, Variation_113385 and Variation_42978, in the Database of Genetic Variants (http://projects.tcag.ca/variation/). The Variation_113385 was analyzed using the TaqMan real-time PCR assay (Applied Biosystems Assay ID, Hs03806891_cn) as previously described (Watanabe et al., 2010b). The Variation_42978 was genotyped, based on the PCR product size. Forward and reverse primer sequences for amplification were 5′-CTGCATTGCCCACTATGTTC-3′ and 5′-CCCAACCATCTTCTTTCTGC-3′, respectively.

Genotypic associations were tested using the Cochran–Armitage test for trend or the Fisher's exact test. Allelic associations were tested using the χ^2 test or the Fisher's exact test. Power calculation was performed using Genetic Power Calculator (http://pngu.mgh.harvard.edu/~purcell/gpc/). Power was estimated using $\alpha = 0.05$, assuming a disease prevalence of 0.01.

We examined 18 SNPs (Table 1) and 2 CNVs (Supplementary Table 4) in the screening population; order and physical locations are shown in Supplementary Fig. 1. We observed potential associations between schizophrenia and three SNPs: rs2129575, rs1487275, and rs17110747 (allelic $p = 0.0117$, 0.0032, and 0.0130, respectively). The rare missense variation rs139896303 (p.R225Q) was detected in two patients as heterozygotes, but not in controls, although the association was not significant. In the confirmatory population, these four SNPs were not significantly associated with schizophrenia (Table 1).

Common *TPH2* SNPs have been tested for associations with schizophrenia (De Luca et al., 2005; Higashi et al., 2007; Shiroiwa et al., 2010; Tee et al., 2010; Kim and Yoon, 2011; Serretti et al., 2011; Zhang et al., 2011). However, previous studies failed to detect significant associations due to the relatively small sample sizes ($n = 70$–720). The present study investigated associations between tagging SNPs and schizophrenia in a Japanese population using two-stage design. In the moderate-scale screening population ($n = 1246$), three common SNPs were demonstrated to be potentially associated with schizophrenia. However, it was not possible to replicate these associations in a large-scale confirmatory population ($n = 4202$). Taken together, these findings suggest that common *TPH2* SNPs do not confer increased susceptibility to schizophrenia.

To the best of our knowledge, no studies have tested rare missense variations of *TPH2* for associations with schizophrenia. The present study resequenced *TPH2* coding regions in 101 patients and detected rs78162420 (p.S41Y). Of note, rs78162420 (p.S41Y) decreases the ability of TPH2 to synthesize serotonin (Lin et al., 2007). This functional variation was not associated with schizophrenia in the screening population.

In addition, rs139896303 (p.R225Q) was examined. In the combined population comprising the screening and confirmatory populations, the Q allele frequencies were 5/5126 in patients and 1/5396 in controls. However, the association was not significant (odds ratio = 5.29, 95% confidence interval = 0.62–45.3). Because the risk allele frequency was extremely low, even a large sample size in the combined population might not provide adequate power to detect an association between rs139896303 (p.R225Q) and schizophrenia. If the genotypic relative risk is set to 5 for heterozygous risk allele carriers under the multiplicative model of inheritance, approximately 6850 patients and 6850 controls are needed to adequately detect the association with a power of 0.80. Further studies should be performed using sufficiently large sample sizes.

Two common intronic CNVs of *TPH2* were not associated with schizophrenia in the screening population. These results did not

0920-9964/$ – see front matter
doi:10.1016/j.schres.2012.01.034

Table 1
Genotype and allele frequencies of SNPs in the screening and confirmatory populations.

Population	Allele [a]	Patients					Controls					*p*	
dbSNP ID		*n*	1/1 [b]	1/2 [b]	2/2 [b]	MAF	*n*	1/1 [b]	1/2 [b]	2/2 [b]	MAF	Genotype	Allele
Screening													
rs7963717	A/C	625	500	118	7	0.106	618	488	125	5	0.109	0.7683	0.7705
rs11178999	A/G	625	162	297	166	0.503	618	171	298	149	0.482	0.3051	0.2950
rs78162420	C/A	614	566	45	3	0.042	620	566	52	2	0.045	0.6660	0.6579
rs4565946	C/T	626	255	285	86	0.365	619	278	270	71	0.333	0.0948	0.0917
rs2129575	T/G	626	138	309	179	0.533	619	177	287	155	0.482	0.0135	0.0117
rs1386488	A/C	626	516	102	8	0.094	618	518	97	3	0.083	0.3414	0.3386
rs17110489	T/C	626	279	275	72	0.335	619	259	270	90	0.363	0.1384	0.1314
rs139896303	G/A	620	618	2	0	0.002	618	618	0	0	0.000	0.4996 [c]	0.4998 [c]
rs17110566	G/A	626	463	154	9	0.137	618	468	139	11	0.130	0.5990	0.6019
rs11179027	G/C	626	220	293	113	0.415	618	186	313	119	0.446	0.1165	0.1154
rs4760820	C/G	624	488	128	8	0.115	618	475	138	5	0.120	0.7319	0.7361
rs1386498	G/A	473 [d]	187	227	59	0.365	457 [d]	188	201	68	0.369	0.8581	0.8574
rs11179043	G/C	625	475	139	11	0.129	618	462	149	7	0.132	0.8178	0.8198
rs12231356	C/T	625	522	98	5	0.086	617	529	86	2	0.073	0.2131	0.2153
rs1487275	A/C	624	360	231	33	0.238	617	310	256	51	0.290	0.0031	0.0032
rs11179059	C/T	626	234	282	110	0.401	620	189	323	108	0.435	0.0882	0.0879
rs11179064	G/A	623	403	187	33	0.203	617	405	192	20	0.188	0.3518	0.3450
rs17110747	G/A	625	404	187	34	0.204	619	353	228	38	0.246	0.0150	0.0130
Confirmatory													
rs2129575	T/G	1974	561	959	454	0.473	2167	552	1092	523	0.493	0.0645	0.0634
rs139896303	G/A	1942	1939	3	0	0.0008	2080	2079	1	0	0.0002	0.3585 [c]	0.3117 [c]
rs1487275	A/C	1877	1005	745	127	0.266	2040	1075	810	155	0.275	0.4020	0.4034
rs17110747	G/A	1833	1117	638	82	0.218	2066	1241	724	101	0.224	0.4923	0.4947

Abbreviations: MAF, minor allele frequency; SNP, single nucleotide polymorphism.
[a] Major/minor allele.
[b] Genotypes, major and minor alleles are denoted by 1 and 2, respectively.
[c] Calculated using the Fisher's exact test.
[d] Individuals without the deleted allele of Variation_42978.

exclude the possibility that other *TPH2* CNVs – in particular rare, but highly penetrant, CNVs – may play a role in schizophrenia pathogenesis. However, recent genome-wide association studies of CNVs did not detect rare *TPH2* CNVs with large effects on schizophrenia risk (Levinson et al., 2011). These findings suggest that *TPH2* CNVs do not contribute to genetic susceptibility to schizophrenia.

In conclusion, our two-stage case–control study suggests that *TPH2* does not confer an increased susceptibility to schizophrenia in the Japanese population.

Supplementary materials related to this article can be found online at doi:10.1016/j.schres.2012.01.034.

References

Abi-Dargham, A., 2007. Alterations of serotonin transmission in schizophrenia. Int. Rev. Neurobiol. 78, 133–164.

De Luca, V., Likhodi, O., Van Tol, H.H.M., Kennedy, J.L., Wong, A.H.C., 2005. Tryptophan hydroxylase 2 gene expression and promoter polymorphisms in bipolar disorder and schizophrenia. Psychopharmacology 183 (3), 378–382.

Egawa, J., Watanabe, Y., Nunokawa, A., Endo, E., Kaneko, K., Tamura, R., Someya, T., 2011. A detailed association analysis between the tryptophan hydroxylase 2 (*TPH2*) gene and autism spectrum disorders in a Japanese population. Psychiatry Res.10.1016/j.psychres.2011.09.001

Higashi, S., Ohnuma, T., Shibata, N., Higashi, M., Matsubara, Y., Arai, H., 2007. No genetic association between tryptophan hydroxylase 2 gene polymorphisms and Japanese schizophrenia. Psychiatr. Genet. 17 (2), 123.

Kim, Y.K., Yoon, H.K., 2011. Effect of serotonin-related gene polymorphisms on pathogenesis and treatment response in Korean schizophrenic patients. Behav. Genet. 41 (5), 709–715.

Levinson, D.F., Duan, J., Oh, S., Wang, K., Sanders, A.R., Shi, J., Zhang, N., Mowry, B.J., Olincy, A., Amin, F., Cloninger, C.R., Silverman, J.M., Buccola, N.G., Byerley, W.F., Black, D.W., Kendler, K.S., Freedman, R., Dudbridge, F., Pe'er, I., Hakonarson, H., Bergen, S.E., Fanous, A.H., Holmans, P.A., Gejman, P.V., 2011. Copy number variants in schizophrenia: confirmation of five previous findings and new evidence for 3q29 microdeletions and VIPR2 duplications. Am. J. Psychiatry 168 (3), 302–316.

Lin, Y.M., Chao, S.C., Chen, T.M., Lai, T.J., Chen, J.S., Sun, H.S., 2007. Association of functional polymorphisms of the human tryptophan hydroxylase 2 gene with risk for bipolar disorder in Han Chinese. Arch. Gen. Psychiatry 64 (9), 1015–1024.

Nunokawa, A., Watanabe, Y., Kaneko, N., Sugai, T., Yazaki, S., Arinami, T., Ujike, H., Inada, T., Iwata, N., Kunugi, H., Sasaki, T., Itokawa, M., Ozaki, N., Hashimoto, R., Someya, T., 2010. The *dopamine D3 receptor* (*DRD3*) gene and risk of schizophrenia: case–control studies and an updated meta-analysis. Schizophr. Res. 116 (1), 61–67.

Serretti, A., Chiesa, A., Porcelli, S., Han, C., Patkar, A.A., Lee, S.J., Park, M.H., Pae, C.U., 2011. Influence of TPH2 variants on diagnosis and response to treatment in patients with major depression, bipolar disorder and schizophrenia. Psychiatry Res. 189 (1), 26–32.

Shiroiwa, K., Hishimoto, A., Mouri, K., Fukutake, M., Supriyanto, I., Nishiguchi, N., Shirakawa, O., 2010. Common genetic variations in *TPH1/TPH2* genes are not associated with schizophrenia in Japanese population. Neurosci. Lett. 472 (3), 194–198.

Tee, S.F., Chow, T.J., Tang, P.Y., Loh, H.C., 2010. Linkage of schizophrenia with TPH2 and 5-HTR2A gene polymorphisms in the Malay population. Genet. Mol. Res. 9 (3), 1274–1278.

Walther, D.J., Peter, J.-U., Bashammakh, S., Hörtnagl, H., Voits, M., Fink, H., Bader, M., 2003. Synthesis of serotonin by a second tryptophan hydroxylase isoform. Science 299 (5003), 76.

Watanabe, Y., Muratake, T., Kaneko, N., Nunokawa, A., Someya, T., 2006. No association between the *brain-derived neurotrophic factor* gene and schizophrenia in a Japanese population. Schizophr. Res. 84 (1), 29–35.

Watanabe, Y., Nunokawa, A., Kaneko, N., Someya, T., 2010a. A case–control association analysis of *CABIN1* with schizophrenia in a Japanese population. J. Hum. Genet. 55 (3), 179–181.

Watanabe, Y., Nunokawa, A., Kaneko, K., Someya, T., 2010b. A case–control study and meta-analysis of association between a common copy number variation of the *glutathione S-transferase mu 1* (*GSTM1*) gene and schizophrenia. Schizophr. Res. 124 (1–3), 236–237.

Zhang, C., Li, Z., Shao, Y., Xie, B., Du, Y., Fang, Y., Yu, S., 2011. Association study of tryptophan hydroxylase-2 gene in schizophrenia and its clinical features in Chinese Han population. J. Mol. Neurosci. 43 (3), 406–411.

Yuichiro Watanabe[1]

Department of Psychiatry, Niigata University Graduate School of Medical and Dental Sciences, 757 Asahimachidori-ichibancho, Chuo-ku, Niigata 951-8510, Japan

Health Administration Center, Headquarters for Health Administration, Niigata University, 8050 Ikarashi-ninocho, Nishi-ku, Niigata 950-2181, Japan

Corresponding author at: Department of Psychiatry, Niigata University Graduate School of Medical and Dental Sciences, 757 Asahimachidori-ichibancho, Chuo-ku, Niigata 951-8510, Japan. Tel.: +81 25 227 2213; fax: +81 25 227 0777.

E-mail address: yuichiro@med.niigata-u.ac.jp(Y. Watanabe).

[1] These authors contributed equally to this work.

Jun Egawa[1]
Department of Psychiatry, Niigata University Graduate School of Medical and Dental Sciences, 757 Asahimachidori-ichibancho, Chuo-ku, Niigata 951-8510, Japan

Yoshimi Iijima
Department of Medical Genetics, Doctoral Program in Social and Environmental Medicine, Graduate School of Comprehensive Human Sciences, University of Tsukuba, 1-1-1 Tennodai, Tsukuba, Ibaraki 305-8575, Japan

Ayako Nunokawa
Naoshi Kaneko
Masako Shibuya
Department of Psychiatry, Niigata University Graduate School of Medical and Dental Sciences, 757 Asahimachidori-ichibancho, Chuo-ku, Niigata 951-8510, Japan

Tadao Arinami
Department of Medical Genetics, Doctoral Program in Social and Environmental Medicine, Graduate School of Comprehensive Human Sciences, University of Tsukuba, 1-1-1 Tennodai, Tsukuba, Ibaraki 305-8575, Japan

Hiroshi Ujike
Department of Neuropsychiatry, Okayama University, Graduate School of Medicine, Dentistry and Pharmaceutical Sciences, 2-5-1 Shikata-cho, Okayama 700-8558, Japan

Toshiya Inada
Seiwa Hospital, Institute of Neuropsychiatry, 91 Bentencho, Shinjuku-ku, Tokyo 162-0851, Japan
Nakao Iwata
Department of Psychiatry, Fujita Health University School of Medicine, Toyoake, Aichi 470-1192, Japan

Mamoru Tochigi
Department of Neuropsychiatry, Graduate School of Medicine, The University of Tokyo, 7-3-1 Hongo, Bunkyo-ku, Tokyo 113-8655, Japan

Hiroshi Kunugi
Department of Mental Disorder Research, National Institute of Neuroscience, National Center of Neurology and Psychiatry, 4-1-1 Ogawahigashi, Kodaira, Tokyo 187-8502, Japan

Masanari Itokawa
Project for Schizophrenia and Affective Disorders Research, Tokyo Metropolitan Institute of Medical Science, 2-1-6 Kamikitazawa, Setagaya-ku, Tokyo 156-8506, Japan

Norio Ozaki
Department of Psychiatry, School of Medicine, Nagoya University, 65 Tsurumai-cho, Showa-ku, Nagoya, Aichi 466-8550, Japan

Ryota Hashimoto
Molecular Research Center for Children's Mental Development, United Graduate School of Child Development, Osaka University, Kanazawa University and Hamamatsu University School of Medicine, D3, 2-2, Yamadaoka, Suita, Osaka, 565-0871, Japan

Toshiyuki Someya
Department of Psychiatry, Niigata University Graduate School of Medical and Dental Sciences, 757 Asahimachidori-ichibancho, Chuo-ku, Niigata 951-8510, Japan

26 December 2011

The American Journal of Pathology, Vol. 179, No. 6, December 2011

DOI: 10.1016/j.ajpath.2011.08.023

Cell Injury, Repair, Aging, and Apoptosis

Glyoxalase I Retards Renal Senescence

Yoichiro Ikeda,* Reiko Inagi,* Toshio Miyata,† Ryoji Nagai,‡ Makoto Arai,§ Mitsuhiro Miyashita,§ Masanari Itokawa,§ Toshiro Fujita,* and Masaomi Nangaku*

From the Division of Nephrology and Endocrinology, Graduate School of Medicine, the University of Tokyo, Tokyo; the United Centers for Advanced Research and Translational Medicine,† Graduate School of Medicine, Tohoku University, Miyagi; the Department of Food and Nutrition,‡ Laboratory of Biochemistry and Nutritional Science, Japan Women's University, Tokyo; and the Tokyo Institute of Psychiatry,§ Tokyo, Japan*

Although kidney functions deteriorate with age, little is known about the general morphological alterations and mechanisms of renal senescence. We hypothesized that carbonyl stress causes senescence and investigated the possible role of glyoxalase I (GLO1), which detoxifies precursors of advanced glycation end products in the aging process of the kidney. We observed amelioration of senescence in GLO1-transgenic aged rats (assessed by expression levels of senescence markers such as p53, $p21^{WAF1/CIP1}$, and $p16^{INK4A}$) and a positive rate of senescence-associated β-galactosidase (SABG) staining, associated with reduction of renal advanced glycation end product accumulation (estimated by the amount of carboxyethyl lysine). GLO1-transgenic rats showed amelioration of interstitial thickening (observed as an age-related presentation in human renal biopsy specimens) and were protected against age-dependent decline of renal functions. We used GLO1 overexpression or knockdown in primary renal proximal tubular epithelial cells to investigate the effect of GLO1 on cellular senescence. Senescence markers were significantly upregulated in renal proximal tubular epithelial cells at late passage and in those treated with etoposide, a chemical inducer of senescence. GLO1 cellular overexpression ameliorated and knockdown enhanced the cellular senescence phenotypes. Furthermore, we confirmed the association of decreased GLO1 enzymatic activity and age-dependent deterioration of renal function in aged humans with GLO1 mutation. These findings indicate that GLO1 ameliorates carbonyl stress to retard renal senescence. ***(Am J Pathol 2011, 179:2810–2821; DOI: 10.1016/j.ajpath.2011.08.023)***

Prevention of aging and increase in longevity have long been dreamt of, and many hypotheses to explain the complex process of aging have been advanced. Primary somatic cells grown *in vitro* do not proliferate indefinitely; rather, after a period of rapid proliferation, the cell division rate slows and ultimately ceases altogether, with the cells becoming unresponsive to mitogenic stimuli, a phenomenon known as replicative senescence or Hayflick's limit. Senescent cells have characteristic features, notably the accumulation of advanced glycation end products (AGEs), wide changes in gene expression (including up-regulation of cell cycle regulators such as p53, $p21^{WAF1/CIP1}$, and $p16^{INK4A}$), and increased senescence-associated β-galactosidase (SABG) activity.[1,2] Irrespective of chronological aging, cells exhibiting the combination of these features are considered to be in premature senescence.[3]

The mechanisms of senescence have been widely investigated. The free radical theory of aging proposes that endogenous reactive oxygen species (ROS) generated in cells result in cumulative damage and subsequent senescence.[4] However, attempts to induce longevity by eliminating oxidative stress in genetically engineered mice have been unsuccessful, suggesting that involvement of free radicals is not a sufficient explanation of senescence.[5,6] Another possible mechanism accounting for senescence is carbonyl stress and AGE formation. Carbonyl compound derivatives are generated by carbohydrate oxidation and glycolysis.[7] AGE formation is caused by carbonyl compound derivatives as protein modification precursors.[8,9] Among the many carbonyl derivatives, the most reactive are thought to be glyoxal and methylglyoxal, which act as protein modification precursor and synergistically contribute to AGE formation.[10] Serum AGE levels were reported to increase with age in a large cohort of normal subjects, and correlated well with levels of established markers of oxidative stress and inflammation.[11] AGE accumulation is associated with the development of age-related diseases, such as diabetes

Supported by Grant-in-Aid for Scientific Research 22590880 (R.I.) and 2139036 (M.N.) from the Japan Society for the Promotion of Science.

Accepted for publication August 24, 2011.

Address reprint requests to Masaomi Nangaku, M.D., Ph.D., Division of Nephrology and Endocrinology, University of Tokyo School of Medicine, 7-3-1 Hongo, Bunkyo-ku, Tokyo, Japan, 113-8655. E-mail: mnangaku-tky@umin.ac.jp.

mellitus, Alzheimer's disease, and atherosclerosis,[12,13] and carbonyl stress is likely to be, at least in part, a cause rather than a consequence of the aging process.[14]

Assuming that glyoxal and methylglyoxal accelerate senescence, acceleration of their decomposition might prevent organs from aging. Both compounds are rapidly decomposed by GLO1 and GLO2, the two enzymes of the glyoxalase (GLO) system. GLO1 catalyzes the conversion of glyoxal and methylglyoxal and reduces glutathione (GSH) to *S*-D-lactoyl-GSH; it is expressed ubiquitously in most tissues, serving as the rate-limiting enzyme of methylglyoxal catabolism.[15–18] In one study, overexpression of GLO1 protected the kidney against ischemia and reperfusion injury by inhibiting the formation of intracellular methylglyoxal adducts and oxidative stress.[19]

In the present study, we investigated the possible roles of carbonyl stress and of GLO1 in renal senescence.

Materials and Methods

Animal Experimental Protocol

Male Wistar rats [wild type (WT)] and male transgenic Wistar rats overexpressing human GLO1 (Tg-GLO1) were used. The Tg-GLO1 rats were generated as described previously.[19,20] Rats 10 weeks of age or 14 months of age were fed a standard moderate-fat diet and tap water *ad libitum* (32 total; $n = 8$ for each age/genotype combination). Food intake was monitored from 2 weeks before sacrifice, and body weight was measured at the time of sacrifice. Systolic blood pressure of awake rats was measured by the tail-cuff method using a Softron BP-98A unit (Softron, Tokyo, Japan). All animal experiments were performed in accordance with the NIH guidelines (7th edition) for use and care of laboratory animals and were approved by the local ethical committees.

Histological Analysis for Age-Related Morphological Change

Tissues from rat and human kidney were fixed in formalin solution and paraffin-embedded. Sections (3 μm thick) were stained with Masson's trichrome staining for rat tissue or with Azan staining for human tissue. Interstitial thickness was measured at a magnification of ×600 as the smallest width of the interstitial area (stained blue) between two intact tubules in 20 sites selected randomly from six fields of renal cortex. This smallest-width measurement was chosen to account for tubules not perpendicular to the cutting plane.

Human renal biopsy specimens obtained from patients admitted to the University of Tokyo Hospital were reviewed with institutional permission (Graduate School of Medicine, University of Tokyo, Permission no. 2671) and with informed consent. Exclusion criteria included confounding factors such as proteinuria [urinary protein > 1 g/g creatinine (Cr)], renal dysfunction (estimated glomerular filtration rate eGFR < 60 mL/min per 1.73 m^2), interstitial nephritis of primary or secondary origin, and diabetes mellitus. The human renal biopsy specimens were mostly from patients with IgA nephropathy, and comparison of glomerular change was not performed because this variable was dependent on disease activity. In all, 22 patients were recruited.

Chemical Analysis

Creatinine concentration was measured by the enzyme method using a Kainos Cre kit (Kainos Laboratories, Tokyo, Japan). Protein concentration was measured by the Lowry method, using DC protein assay reagents (Bio-Rad Laboratories, Hercules, CA). Rat blood or urine samples collected for 24 hours in metabolic cages were used after centrifugation for 5 minutes at 3000 × *g*. Blood glucose level was measured using an automated blood glucose meter (Glutest Ace; Sanwa Chemical, Nagoya, Japan). Blood insulin level was measured using a rat insulin ELISA kit (AKRIN-010T; Shibayagi, Gunma, Japan). HbA1c was measured by high performance liquid chromatography.

Determination of GLO1 Activity and GSH Concentrations

Renal cortex of rats (30 mg) or 10^4 to 10^5 renal proximal tubular epithelial cells (RPTECs) were homogenized in, respectively, 0.5 mL or 50 μL of sodium phosphate buffer, pH 7.0, containing 0.02% Triton X-100 surfactant, then sonicated for 1 minute, and finally centrifuged at 20,000 × *g* for 1 minute at 4°C. The supernatant was used for assessment of GLO1 activity by spectrophotometry, as described previously.[21] GSH concentration in renal cortical homogenates from rats was measured with Bioxytech GSH-412 assay reagent (Oxis International, Portland, OR). Values were adjusted by the protein concentration of the same sample.

Determination of Total Superoxide Dismutase Activity

Total superoxide dismutase (SOD) activity in renal tissue was determined using a superoxide dismutase assay kit (Cayman Chemical, Ann Arbor, MI). Sample preparation and measurement were performed according to the manufacturer's instructions. Values were adjusted by the protein concentration of the same sample.

Senescence-Associated β-Galactosidase Staining Assay

Staining for senescence-associated β-galactosidase (SABG), one of the senescence markers, was performed using a Chemicon cellular senescence assay kit (Millipore, Billerica, MA). For tissue staining, frozen 15-μm kidney sections were incubated for 5 hours. The SABG-positive (blue-stained) areas of whole renal cortex were measured at ×100 magnification. The SABG-positive rate of tissue was calculated using ImageJ software (version 1.38) (NIH, Bethesda, MD) with adequate setting of threshold and computed measurement of area fraction,

obtained after analyzing particles. Eight areas of each kidney section were used for statistical assessment. For costaining of SABG staining and γ-GTP staining or immunohistochemical staining, frozen 10-μm kidney sections were used. SABG staining, with 12 hours of incubation, was performed prior to immunohistochemical staining.

Immunoblot Analysis

Proteins were separated by 10% to 15% SDS-PAGE under reducing conditions. Monoclonal mouse anti-p53 IgG (Calbiochem Ab-1, 1:100; EMD Chemicals, Cambridge, MA), monoclonal mouse anti-$p16^{INK4A}$ IgG (sc-1661, 1:200; Santa Cruz Biotechnology, Santa Cruz, CA), monoclonal mouse anti-CEL IgG (1:100),[22] and polyclonal rabbit anti-β actin IgG (A2066, 1:1000; Sigma-Aldrich, St. Louis, MO) were used as primary antibodies, and horseradish peroxidase-conjugated anti-mouse or anti-rabbit IgG (170–6516 for anti-mouse and 170–6516 for anti-rabbit, 1:1000; Bio-Rad Laboratories) were used as secondary antibodies. The ECL Plus Western blotting system (GE Healthcare, Piscataway, NJ) was used for detection. Reproducibility was confirmed in three independent experiments; representative data are presented in the figures.

Immunohistochemistry

The following primary antibodies were used: polyclonal rabbit anti-GLO1 IgG (12 μg/mL, obtained from immunization against synthetic peptide of rat GLO1, GIAVPDVYEA, which cross-reacts with the human GLO1 epitope, GIAVPDVYSA); anti-aquaporin2 (AQP2) IgG (Chemicon AB3274) from Millipore; anti-p53 IgG (sc-6243), monoclonal mouse anti-$p21^{WAF1/CIP1}$ IgG (sc-6246), and anti-$p16^{INK4A}$ IgG (sc-1661) from Santa Cruz Biotechnology; and anti-calbindin-D-28K IgG (c-9848) from Sigma-Aldrich. Polyclonal horse biotinylated anti-mouse IgG antibody or polyclonal goat anti-rabbit IgG (Vector Laboratories, Burlingame, CA) was used as secondary antibody. Reproducibility was confirmed in three independent experiments; representative data are reported in the results.

Real-Time Quantitative PCR

The primers used for real-time quantitative PCR were as follows: human GLO1 5′-ATTCGGTCATATTGGAATTGC-3′ (forward), 5′-TTCAATCCAGTAGCCATCAGG-3′ (reverse); human p53 5′-CCTCACCATCATCACACTGG-3′ (forward), 5′-TCTGAGTCAGGCCCTTCTGT-3′ (reverse); human $p21^{WAF1/CIP1}$ 5′-TGGAGACTCTCAGGGTCGAAA-3′ (forward), 5′-GGCGTTTGGAGTGGTAGAAATC-3′ (reverse); human $p16^{INK4A}$ 5′-CAACGCACCGAATAGTTACG-3′ (forward), 5′-AGCACCACCAGCGTGTC-3′ (reverse); human β-actin 5′-TCCCCCAACTTGAGATGTATGAAG-3′ (forward), 5′-AACTGGTCTCAAGTCAGTGTACAGG-3′ (reverse); rat p53 5′-CCTCAATAAGCTGTTCTGCC-3′ (forward), 5′-AAAAGTCTGCCTGTCGTCCA-3′ (reverse); rat $p21^{WAF1/CIP1}$ 5′-ACGTGGCCTTGTCGCTGTCTT-3′ (forward), 5′-TAAGGCAGAAGATGGGGAAGAG-3′ (reverse); rat $p16^{INK4A}$ 5′-ACGAGGTGCGGGCACTG-3′ (forward), 5′-TTGACGTTGCCCATCATCATC-3′ (reverse); rat β-actin 5′-CTTTCTACAATGAGCTGCGTG-3′ (forward), 5′-TCATGAGGTAGTCTGTCAGG-3′ (reverse); rat Mn-SOD 5′-CCGAGGAGAAGTACCACGAG-3′ (forward), 5′-GCTTGATAGCCTCCAGCAAC-3′ (reverse). Amplification specificity was verified by agarose gel electrophoresis of the PCR products. Expression data were normalized to β-actin using the ΔΔCt method.

Cell Culture

Primary human RPTECs derived from a 27-year-old woman of European origin were purchased from Clonetics (Walkersville, MD). The cells were cultured with renal epithelial basal medium (Clonetics). Early- and late-passage cells were compared at passages 3 and 10, respectively, and cells of passage 3 to 4 were used for transfection experiments. Confluent RPTEC monolayers were passaged at 1:4. Each experiment with RPTECs was performed three or more times independently.

Transfection

cDNA of human GLO1 (555 bp) was obtained using the following primers: 5′-CAGGCTAGCCATGGCAGAACCGCAGCC-3′ (forward), 5′-GGAGAATTCTCACAGCACTACATTAAG-3′ (reverse). Plasmid vector pcDNA3.1(−) (Invitrogen, Carlsbad, CA) was used for overexpression of GLO1. GLO1 containing pcDNA3.1(−) was constructed by inserting the complete human form GLO1 cDNA into the EcoRI and NheI sites. For overexpression experiments, 400 ng/cm^2 of GLO1-containing vector or empty vector was transfected into RPTECs by 5 hours of incubation with Lipofectamine 2000 transfection reagent (Invitrogen). Cells were exposed to 1 μmol/L etoposide for 24 hours if necessary. Transfection efficiency was confirmed by transfection of LacZ-containing vector followed by *in situ* β-galactosidase staining solution, using empty vector as control.

Knockdown Study

Knockdown study was performed using Stealth Select RNAi purchased from Invitrogen. Sequences for GLO1 were as follows: 5′-UUAGCGUCAUUCCAAGAACUCUAGU-3′ (siRNA 1), 5′-AAUCCAGUAGCCAUCAGGAUCUUGA-3′ (siRNA 2). Stealth RNAi negative control (universal negative control siRNA) from Invitrogen was used as scrambled siRNA. Knockdown efficiency was confirmed by real-time quantitative PCR with primers of human GLO1.

Cellular Proliferation and Viability Test

The number of viable cells was determined using a colorimetric MTS formazan assay with CellTiter 96 AQ_{ueous} One Solution cell proliferation assay (Promega, Madison, WI). Cells (10^3) were seeded with renal epithelial basal medium, with or without etoposide exposure.

For the lactate dehydrogenase (LDH) assay, 10^4 cells at early or late passage with or without etoposide exposure were seeded into each well of a 24-well plate with renal epithelial basal medium and were incubated for 24 hours. Cells were lysed with 0.1% Triton X-100 surfactant, and 2 μL of cell lysate and 200 μL of culture medium were used for each measurement. LDH activity was measured using a Kainos LDH kit (Kainos Laboratories).

Bromodeoxyuridine (BrdU) uptake was measured using a BrdU detection kit III (Roche Diagnostics, Indianapolis, IN). Cells (10^4) cells at passage 3 were seeded in each well of a 96-well plate and were cultured with serum-free Dulbecco's modified Eagle's medium for 24 hours, with etoposide added after transfection if necessary.

γ-Glutamyl Transpeptidase Staining

γ-Glutamyl transpeptidase (GTP) staining was performed according to the method of Rutenburg et al.[23] Duration of incubation for staining was 10 minutes at room temperature. No fixation was done before staining.

Immunofluorescence Study

Cells were fixed in 50% methanol/50% acetone and then were incubated with anti-CEL antibody (KNH-30; TransGenic, Kobe, Japan) as a primary antibody. Fluorescein isothiocyanate-conjugated polyclonal rabbit anti-mouse IgG (F0261; Dako, Glostrup, Denmark) was used as a secondary antibody. Nuclei were then counterstained with Hoechst 33258 dye (B2883; Sigma-Aldrich).

Renal Function and GLO1 Mutation in Human Schizophrenia Patients

For determination of eGFR, we used data from patients with schizophrenia whose GLO1 genotype had been established previously,[24] with permission and informed consent. The local human ethics committee approved all protocols involving patients, and informed written consent was obtained from every patient before enrollment. Three patients had the GLO1 frameshift mutation, with GLO1 activity half that of the nonmutant form,[24] and 15 age-matched control patients with WT GLO1 were randomly selected. All medical charts were reviewed for blood pressure, body weight, body height, urinary testing (hematuria, proteinuria), and medication. The eGFR was calculated using the following formula, which estimates GFR in a Japanese population[25]: $eGFR = 194 \times Cr^{-1.094} \times Age^{-0.287}$ ($\times$ 0.739 if female).

Statistical Analysis

Data are expressed as means $\pm$ SD. Statistical differences were assessed using the unpaired Student's *t*-test or single-factor analysis of variance. Significant differences determined on analysis of variance were tested by post hoc comparison using Tukey's method. Values of $P < 0.05$ were considered statistically significant. In analysis of human renal biopsy, the slope of interstitial thickness against age was calculated by linear regression analysis with Spearman's rank correlation coefficient.

Results

Amelioration of Senescent Status in Aged Kidneys of Tg-GLO1 Rats

To study the biological roles of carbonyl stress and GLO1 in renal senescence, we used young (10-week-old) and aged (14-month-old) Tg-GLO1 and WT rats (32 total; $n = 8$ for each age/genotype combination).[19,20] No significant differences were seen between the WT and Tg-GLO1 groups, either young or aged, in body weight, food intake per weight, or systolic blood pressure (Table 1). Levels of random (nonfasting) blood glucose did not significantly differ between WT and Tg-GLO1 rats during the experimental period. Normal glucose metabolism in the experimental animals was confirmed by measurements of fasting blood glucose, fasting blood insulin, insulin resistance, and HbA1c. The HOMA-IR (homeostasis model of assessment-insulin resistance) index of insulin resistance was calculated by multiplying fasting blood glucose and fasting blood insulin, then dividing by 405. All of these parameters were equivalent between aged WT and Tg-GLO1 rats (Figure 1, A–E). Similarly, levels of renal cortex GSH, an essential cofactor of GLO1, did not significantly differ between them (Figure 1F). To eliminate the effect of antioxidants, which may ameliorate senescence phenotypes by decreasing ROS levels, total superoxide dismutase (SOD) activity in renal tissue was measured. Total SOD activity was not significantly changed by GLO1 overexpression in either young or aged rats (Figure 1G). In addition, transcript levels of

Table 1. Body Weight, Food Intake, and Systolic Blood Pressure of Young and Elderly Wild-Type and Transgenic Rats

Characteristics	Young		Elderly	
	WT	Tg-GLO1	WT	Tg-GLO1
Body weight (g)	330 ± 17	330 ± 26	490 ± 56*	480 ± 54*
Chow intake (mg/day per g weight)	43 ± 13	42 ± 14	39 ± 12	42 ± 14
Systolic blood pressure (mmHg)	106 ± 4	104 ± 5	106 ± 11	104 ± 9

Significant differences were found in body weight in elderly compared with young rats, but no significant differences were found in those of the same age. No significant differences were observed in food intake or systolic blood pressure; $n = 8$ in each of the four categories.
* $P < 0.01$ versus young WT.

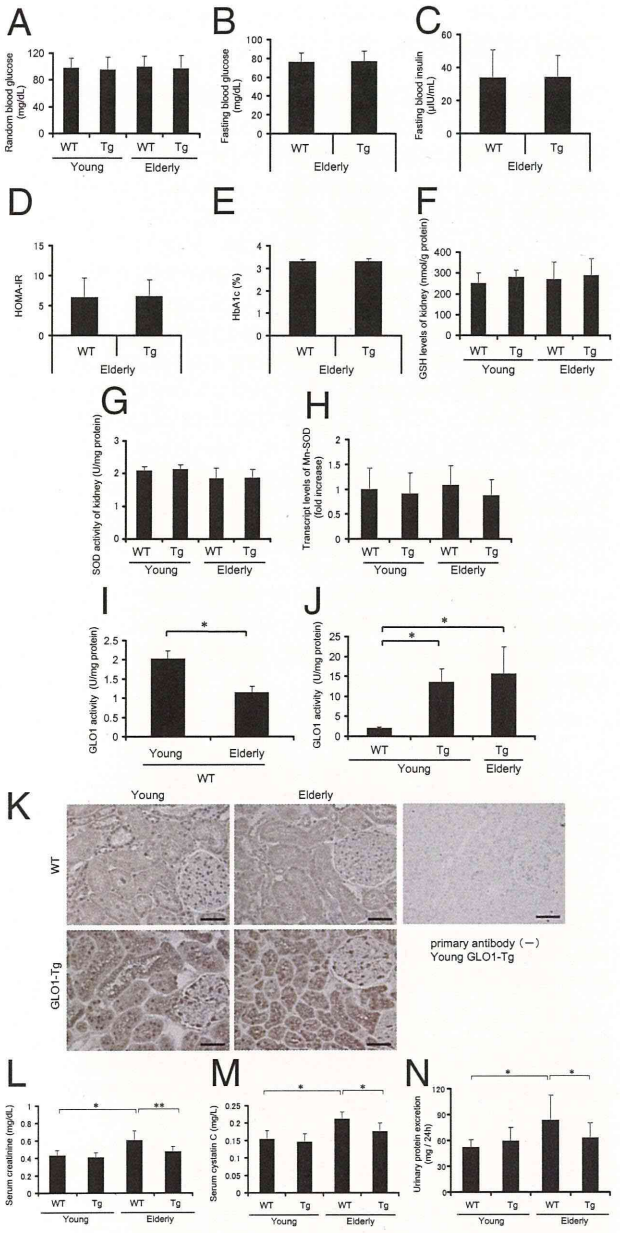

Figure 1. Characteristics of GLO1-overexpressing aged rats and amelioration of senescence-associated renal dysfunction and urinary protein excretion. No significant differences were observed between young and aged WT and Tg-GLO-1 rats for random (nonfasting) blood glucose levels (**A**), for levels of GSH, an essential cofactor of GLO1, in renal cortex lysate (data adjusted by protein concentration) (**F**), for total SOD activity of renal cortex lysate (data adjusted by protein concentration) (**G**), and for relative transcript levels of Mn-SOD (determined by real-time quantitative RT-PCR, with the value for young WT rats set as 1) (**H**). No significant differences were observed between aged WT and Tg-GLO-1 rats for fasting blood glucose levels (**B**), for fasting blood insulin levels (**C**), for HOMA-IR (calculated by multiplying fasting blood glucose and fasting blood insulin, then dividing by 405) (**D**), and for blood HbA1c levels (**E**). **I:** GLO1 activity of renal cortex lysate of WT animals decreased in an age-dependent manner. Data were adjusted by protein concentration. $^{*}P < 0.01$. **J:** GLO1 activity of renal cortex lysate in Tg-GLO1 rats was markedly higher than that in WT rats, and did not show an age-dependent decrease. Data were adjusted by protein concentration. $^{*}P < 0.01$ versus young WT rats. **K:** Distribution of GLO1 in rat kidney, shown in representative micrographs of immunohistochemical staining of GLO1 in the rat renal cortex. GLO1 was expressed ubiquitously in the kidney of both WT and Tg-GLO1 rats. Methyl Carnoy's fixed specimens (4 μm thick) were counterstained with hematoxylin. Original magnification = ×400. Scale bars: 50 μm. **L:** Serum creatinine levels determined by enzymatic assay indicate that the age-dependent deterioration of renal function was ameliorated by GLO1 overexpression. $^{*}P < 0.01$; $^{**}P < 0.05$. **M:** Serum cystatin C levels indicate that the age-dependent deterioration of renal function was ameliorated by GLO1 overexpression. $^{*}P < 0.01$. **N:** An age-dependent increase in proteinuria was prevented by GLO1 overexpression. Urine was collected for 24 hours using metabolic cages. $^{*}P < 0.05$.

manganese SOD (Mn-SOD, or SOD2) in kidney were measured by quantitative RT-PCR; Mn-SOD regulates only mitochondrial production of ROS because it is present only in mitochondria. No significant differences in Mn-SOD expression were observed between young and aged groups of WT and Tg-GLO1 rats (Figure 1H).

In WT rats, GLO1 activity was significantly decreased with age, to 0.55-fold the level in young rats (Figure 1I). GLO1 activity of young Tg-GLO1 rats showed a 6.3-fold increase, compared with young WT rats, but did not show an age-dependent decrease (Figure 1J). Immunohistochemical analysis showed that GLO1 was ubiquitously expressed with the same distribution pattern in the kidneys of both young and aged WT rats (Figure 1K). In contrast to the comparison in WT rats which showed age-dependent weakening of signal intensity, GLO1 signal intensity in Tg-GLO1 did not change with aging. Age-dependent deterioration of renal function, as estimated by serum creatinine, cystatin C levels, and urinary protein excretion, were markedly ameliorated by overexpression of GLO1 (Figure 1, L–N).

We assessed renal senescence status in WT and Tg-GLO1 rats by SABG staining. SABG was positive only in the tubular cells of aged rats; glomerular cells remained negative (Figure 2A). The functional improvement in renal senescence described above in Tg-GLO1 rats was associated with a decrease in SABG-positive rates in cortical tubular cells. Amelioration of senescence was confirmed by quantitative analysis of the SABG-positive rate, which was lower in the kidneys of aged Tg-GLO1 rats, compared with aged WT rats (Figure 2B). No significant differences were observed between the kidneys of young Tg-GLO1 and WT rats. To determine which segments of tubules are positive for SABG staining, we performed costaining of SABG and γ-GTP (a marker of proximal tubular cells), calbindin-D-28K (a marker of distal tubules and connecting tubules), or aquaporin2 (AQP2; a marker of connecting tubules and collecting ducts) (Figure 2, C–E). All segments had a propensity toward senescence, with no preponderance in specific tubular segments. The elevated transcript levels of senescence markers such as p53, $p21^{WAF1/CIP1}$, and $p16^{INK4A}$ in aged rats were significantly suppressed by GLO1 overexpression, compared with aged WT rats, whereas no significant differences were observed between the young groups (Figure 2F). Immunohistochemistry for the senescence markers showed that the nuclei of renal cortical tubules of aged WT rats were stained positive (in staining for p53, cytosol was also positive); these positive staining levels were markedly reduced in aged Tg-GLO1 rats (Figure 2G). Similar results were obtained by immunoblot analysis of renal cortex lysate for p53 and $p16^{INK4A}$. Protein expression level of p53 and $p16^{INK4A}$ in the young rats was undetectable; however, the increased expression of p53 and $p16^{INK4A}$ with age was reduced by GLO1 overexpression (Figure 2, H and I). In parallel with this suppression of senescence markers, age-dependent accumulation of carboxyethyl lysine (CEL) in the renal cortex was markedly suppressed by overexpression of GLO1 (Figure 2J).

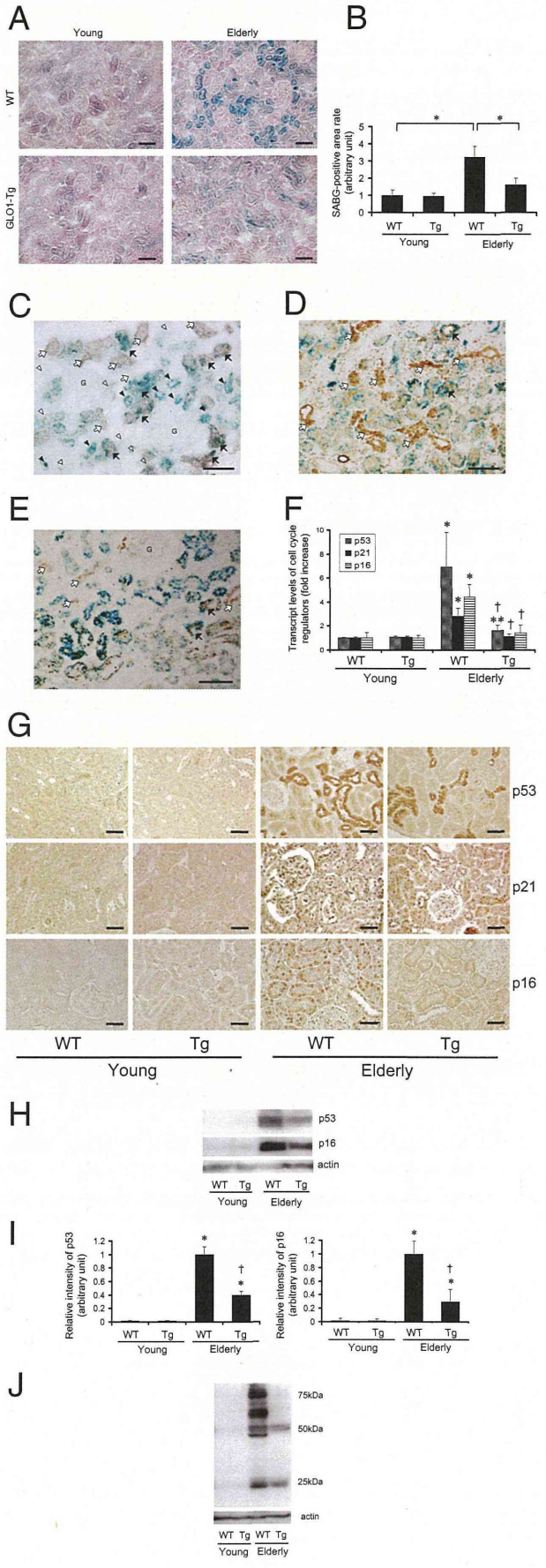

Age-Related Morphological Changes in the Renal Interstitium

To investigate whether amelioration of senescence markers and physiological parameters by overexpression of GLO1 was associated with improvement of pathological changes, we first assessed age-related morphological changes in human renal senescence, with a particular focus on tubulointerstitial changes (Figure 3A), on the basis that SABG staining was observed primarily in the tubules in aged rats. Review of specimens (mostly IgA nephropathy specimens with Azan staining) from 22 patients whose renal functions were preserved (eGFR of 80.4 ± 3.5 mL/min per 1.73m^2 and urinary protein excretion of 0.76 ± 0.21 g/day) showed an age-dependent increase in the thickness of the interstitium (Figure 3B). Linear regression analysis showed a strongly positive Pearson's correlation coefficient between age and the thickness of the renal peritubular interstitium (slope, 0.044 μm/year; $r^2 = 0.91$, $P < 0.01$).

In accord with the findings in humans, we observed tubulointerstitial morphological changes in aged rats. These changes were significantly decreased in aged Tg-GLO1 rats (Figure 3, C and D).

Figure 2. GLO1-overexpressing aged rats showed morphological amelioration in senescence-associated alterations of kidney. **A:** Light micrographs of rat renal cortex with SABG staining showing senescent tubular cells in aged WT rats. The number of senescent tubules was reduced by overexpression of GLO1. Frozen tissue specimens (15 μm thick) were counterstained with Nuclear Fast Red. Original magnification: ×100. Scale bars: 100 μm. Blue indicates SABG-positive cells. **B:** Quantitative analysis of SABG-positive area. The positive rate was calculated by dividing the positive area by the total area in each field and is expressed as fold increase, relative to the level of young WT rats. $^*P < 0.01$. **C:** Representative light micrographs of renal cortex of aged WT rat, costained with SABG (blue) and γ-GTP (pale red). **Black arrows** mark senescent proximal tubular cells; **white arrows** mark nonsenescent proximal tubular cells. **Black arrowheads** mark senescent nonproximal tubular cells; **white arrowheads** mark nonsenescent nonproximal tubular cells. The letter G marks the glomerulus. Frozen specimens were examined without counterstaining. Original magnification = ×200. Scale bar = 100 μm. **D:** Representative light micrographs of renal cortex of aged WT rat costained with SABG (blue) and calbindin-D-28K. **Black arrows** mark senescent distal tubules-connecting tubules; **white arrows** mark nonsenescent distal tubules-connecting tubules. Frozen specimens were counterstained with hematoxylin. Original magnification = ×200. Scale bar = 100 μm. **E:** Representative light micrographs of renal cortex of aged WT rat costained with SABG (blue) and AQP2. **Black arrows** mark senescent connecting tubules-collecting ducts; **white arrows** mark nonsenescent connecting tubule-collecting ducts. The letter G marks the glomerulus. Frozen specimens were counterstained with hematoxylin. Original magnification = ×200. Scale bar = 100 μm. **F:** Relative transcript levels of p53, p21$^{WAF1/CIP1}$, and p16^{INK4A} were determined by real-time quantitative RT-PCR. All were significantly elevated in aged WT. This age-dependent increase was significantly reduced by overexpression of GLO1. The values for young WT rats were set as 1. $^*P < 0.01$; $^{**}P < 0.05$ versus young WT rats; $^{\dagger}P < 0.01$ versus aged WT rats. **G:** Representative micrographs of immunohistochemistry staining for p53, p21$^{WAF1/CIP1}$, and p16^{INK4A} in the rat renal cortex. In each staining, aged WT tissue exhibited marked increases in positive area in tubules. The extent of positive areas was significantly decreased by overexpression of GLO1. Methyl Carnoy's fixed specimens (4 μm thick) were counterstained with hematoxylin. Original magnification = ×400. Scale bars: 50 μm. **H:** Protein immunoblot of p53 and p16^{INK4A} of renal cortex lysate. Elevation of p53 and p16^{INK4A} in aged WT rats was attenuated by overexpression of GLO1. Actin served as a control. **I:** Densitometric quantification of p53 and p16^{INK4A} immunoblot. The values for aged WT rats were set as 1. $^*P < 0.05$ versus young WT rats; $^{\dagger}P < 0.05$ versus aged WT rats. **J:** Protein immunoblot of CEL of renal cortex lysate indicates amelioration of carbonyl stress by GLO1 overexpression. Actin served as a control. Many bands were detected as CEL-modified protein, indicating that AGEs were accumulated in renal cortex.

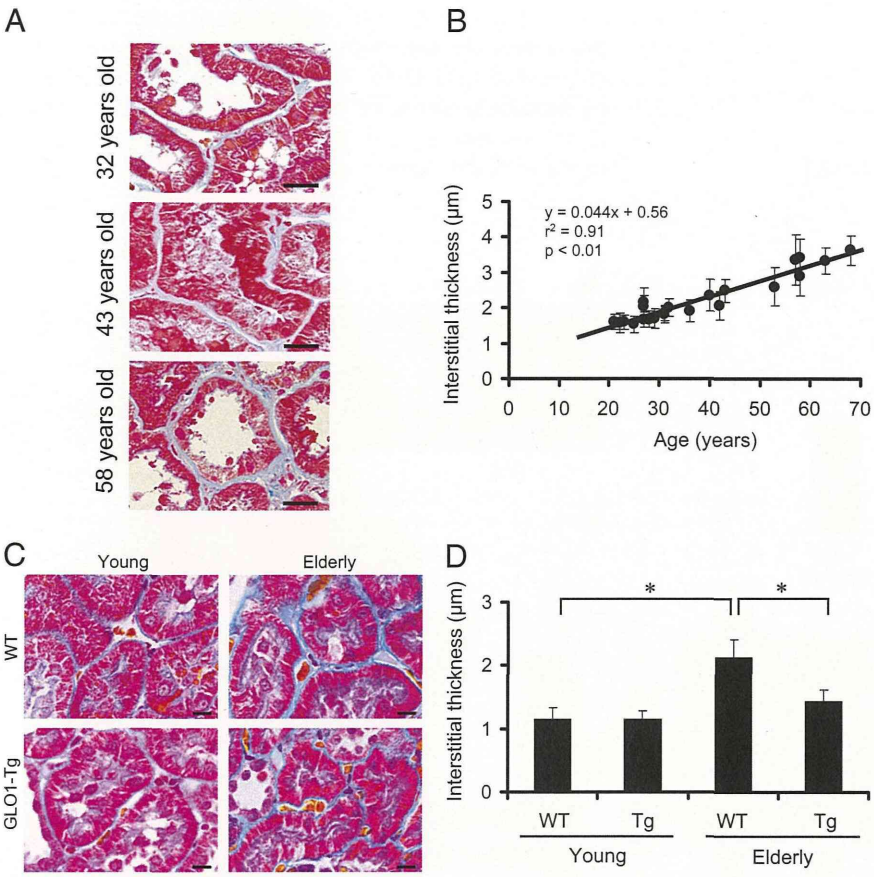

Figure 3. Interstitial thickening was demonstrated to be an age-related morphological change in human and rat kidney. **A:** Representative figures of human renal biopsy. Specimens were Azan-stained. Proximal tubular epithelial cells stain red and interstitium stains blue. The interstitial areas were thickened in an age-dependent manner. Original magnification = ×600. Scale bars: 20 μm. **B:** Correlation between age and interstitial thickness. The thickness of renal interstitia (blue) was measured under high-power magnification (×600). Each dot on the univariate linear regression line represents mean thickness (μm); error bars indicate ± SD. The calculation method is described under *Materials and Methods*. **C:** Light micrographs of rat renal cortex. Formalin-fixed specimens (3 μm thick) were stained with Masson's trichrome staining. Proximal tubular epithelial cells with brush borders stain red; interstitial areas stain blue (as for the human renal biopsy). The interstitial areas were thickened with age. This age-dependent thickening was attenuated by GLO1 overexpression. Original magnification = ×600. Scale bars: 10 μm. **D:** Quantitative histological analysis indicates that GLO1 overexpression ameliorated age-dependent interstitial thickening. $^{*}P < 0.01$; $^{**}P < 0.05$.

Carbonyl Stress and Cellular Senescence in Primary Cultured Tubular Cells

To confirm the significance of carbonyl compound in age-related alterations in tubular cells, we used primary cultured human RPTECs. First, we investigated the senescence status of RPTECs at early and late passage (passage 3 and 10, respectively). Cell proliferation estimated by the MTS assay showed that RPTECs reached replicative senescence at late passage (Figure 4A). Treatment of early-passaged cells with 1 μmol/L etoposide, a chemical senescence inducer, successfully induced replicative senescence, as was observed in late-passaged cells (Figure 4A). The LDH assay revealed no significant differences in cell viability among the three groups (Figure 4B). The cultured cells retained the phenotypes of proximal tubular cells, as evaluated by γ-GTP staining, a specific marker of proximal tubular cells. In contrast, γ-GTP was negative in rat renal fibroblasts (Figure 4C).

We then assessed the change in expression levels of cellular senescence markers in RPTECs at late passage or by etoposide treatment. The number of SABG-positive cells was significantly increased in late-passaged RPTECs and in early-passaged RPTECs treated with etoposide, compared with untreated early-passaged cells, verifying our assumption that the premature senescence induced by this chemical inducer closely mimics cellular senescence (Figure 5, A and B). We further assessed the changes in other senescence markers in the three groups of RPTECs. Transcriptional levels of p53, $p21^{WAF1/CIP1}$, and $p16^{INK4A}$ were significantly increased in late-passaged RPTECs and etoposide-treated early-passaged RPTECs, compared with untreated early-passaged RPTECs (Figure 5C). Immunoblot analysis followed by densitometry revealed the up-regulation of p53 at the protein level in RPTECs in association with replicative senescence (Figure 5, D and E). Immunofluorescent microscopy showed that late-passaged and etoposide-treated early-passaged cells showed accumulation of CEL, an indicator of carbonyl stress status, but untreated early-passaged cells did not (Figure 5F).

Beneficial Effect of GLO1 on Senescence of Tubular Cells

We next used RPTECs treated with etoposide for functional studies. First, we performed gain-of-function studies using early-passaged RPTECs overexpressing human GLO1, which is a detoxifying enzyme of reactive carbonyl compounds, including methylglyoxal. Transfection efficiency in RPTECs as estimated using LacZ expression as a reporter gene was 87 ± 6%, and GLO1 activity was up-regulated by 14 ± 2-fold in GLO1-transfected cells, compared with empty vector-transfected cells (Figure 6A). Overexpression of GLO1 did not change the basal expression level of SABG in these transfectants.

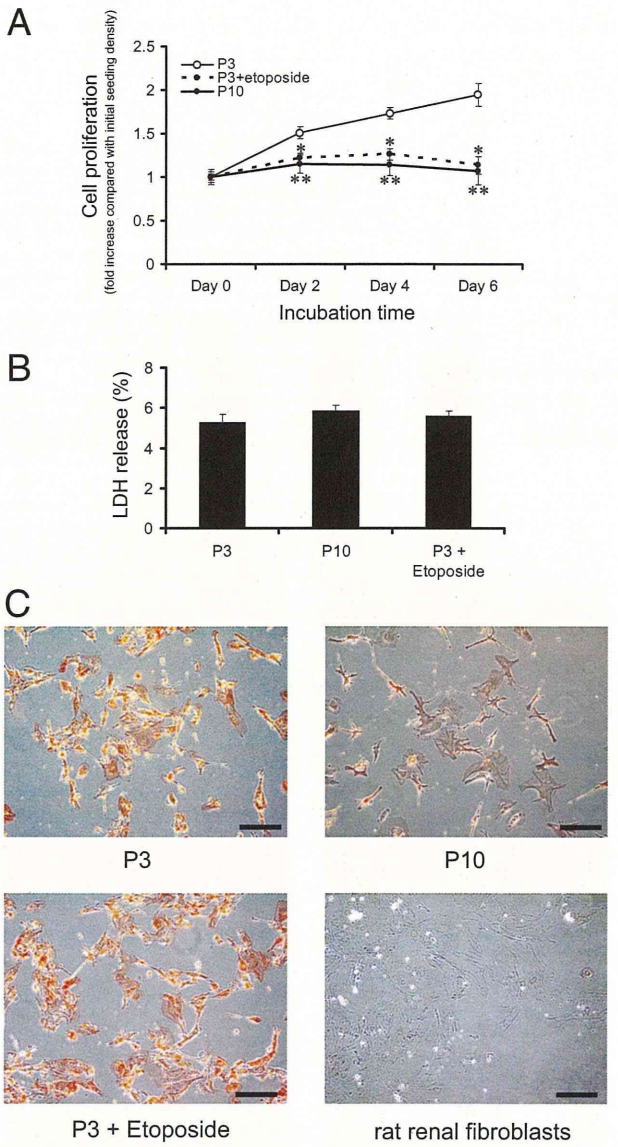

Figure 4. Validation of replicative senescence and senescence induced by etoposide in RPTECs. **A:** Cell proliferation rate determined by MTS assay showed replicative senescence at late passage (P10) and with exposure to a chemical senescence inducer, etoposide, at early passage (P3). Normal RPTECs doubled their population within 1 week, whereas senescent RPTECs and those exposed to etoposide did not proliferate. Assays were made at 2-day intervals, with the value on day 0 set as 1. $^{*}P < 0.01$; $^{**}P < 0.05$ versus day 0 of passage 3. **B:** LDH release was equivalent among RPTECs at passage 3 with or without etoposide exposure and at passage 10, excluding cells in which proliferation was halted because of cytotoxicity. LDH release = LDH in culture supernatant/(LDH in culture supernatant + LDH in cell lysate) ×100. **C:** Phase-contrast light micrographs with γ-GTP staining of RPTECs at passage 3 with or without etoposide exposure and at passage 10 and of rat renal fibroblasts confirmed that the cells retained the phenotype of proximal tubular cells. Original magnification = ×100. Scale bars: 200 μm. Red staining indicates cells positive for γ-GTP activity.

Of note, empty vector-transfected cells treated with etoposide showed a significant increase in SABG-positive cells, by 2.3 ± 1.0-fold, which was significantly suppressed by GLO1 overexpression (Figure 6, B and C). Transcript expression levels of p53, $p21^{WAF1/CIP1}$, and $p16^{INK4A}$, as well as protein expression levels of p53 in whole cellular lysate from etoposide-treated cells, were also significantly decreased in GLO1-transfected cells, compared with empty vector-transfected cells, whereas those without etoposide exposure showed no significant differences (Figure 6, D–F). Accumulation of CEL augmented by etoposide exposure was significantly suppressed by GLO1 overexpression, but remained at the increased levels with transfection of empty vector (Figure 6G).

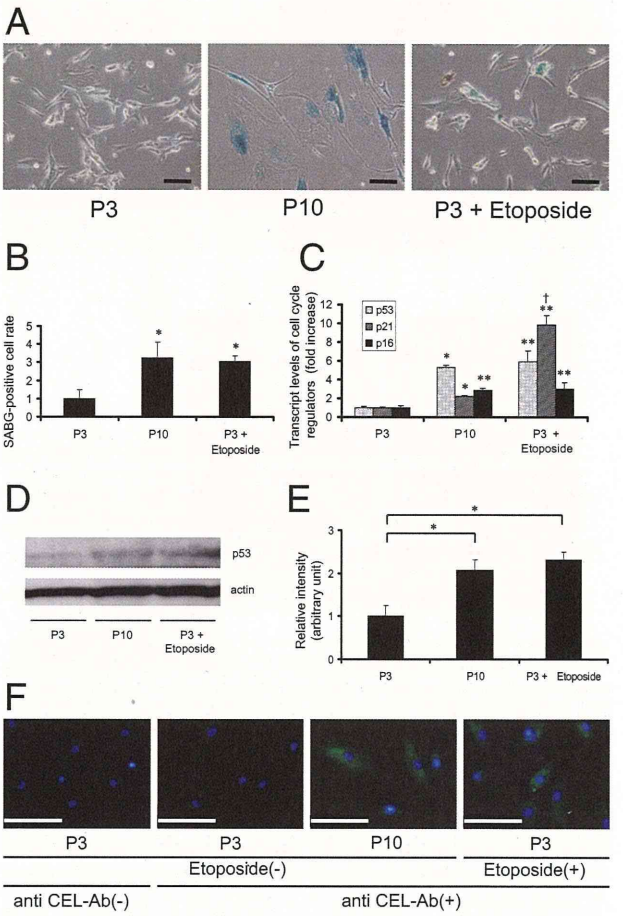

Figure 5. Carbonyl stress and cellular senescence in RPTECs. **A:** Phase-contrast light micrographs with SABG staining of RPTECs at passage 3 with or without etoposide exposure and at passage 10 show senescence of cells at passage 3 with etoposide exposure and at passage 10. Glutaraldehyde fixation was done before staining. SABG staining was performed by incubation for 5 hours without CO_2. Original magnification = ×100. Scale bars: 100 μm. Blue staining indicates positive cells. **B:** Quantitative analysis of SABG-positive cells per total cells in each field. Most RPTECs were senescent at passage 10 or with etoposide exposure. $^{*}P < 0.01$ versus day 0 at passage 3. **C:** Transcript levels of p53, $p21^{WAF1/CIP1}$, and $p16^{INK4A}$ of RPTECs at passage 3 with or without etoposide exposure and at passage 10 determined by real-time quantitative RT-PCR. All showed significant elevation compared with cells at passage 3 without etoposide exposure. Values of those at passage 3 were set as 1. $^{*}P < 0.01$; $^{**}P < 0.05$ versus each at passage 3; $^{\dagger}P < 0.05$ versus $p21^{WAF1/CIP1}$ at passage 10. **D:** Protein immunoblot of p53 of whole lysate of RPTECs at passage 3 with or without etoposide exposure and at passage 10 confirmed the results of real-time quantitative PCR analysis. Cells were lysed in urea buffer under reducing conditions. Actin served as a control. **E:** Densitometric quantification of p53 immunoblot of RPTECs at early passage (P3) with or without etoposide exposure and at late passage (P10). The level of cells at early passage without etoposide exposure was set as 1. $^{*}P < 0.01$ versus cells at passage 3 without etoposide exposure. **F:** Immunofluorescent micrographs for the detection of CEL showed carbonyl stress in senescent RPTECs. Only cells at passage 3 with etoposide exposure and at passage 10 exhibited a cytosolic positive signal. Cells were fixed with methanol 50%:acetone 50%. Green indicates anti-CEL (fluorescein isothiocyanate); blue stain identifies nuclei (Hoechst 33258 dye). Original magnification = ×400. Scale bars: 100 μm.

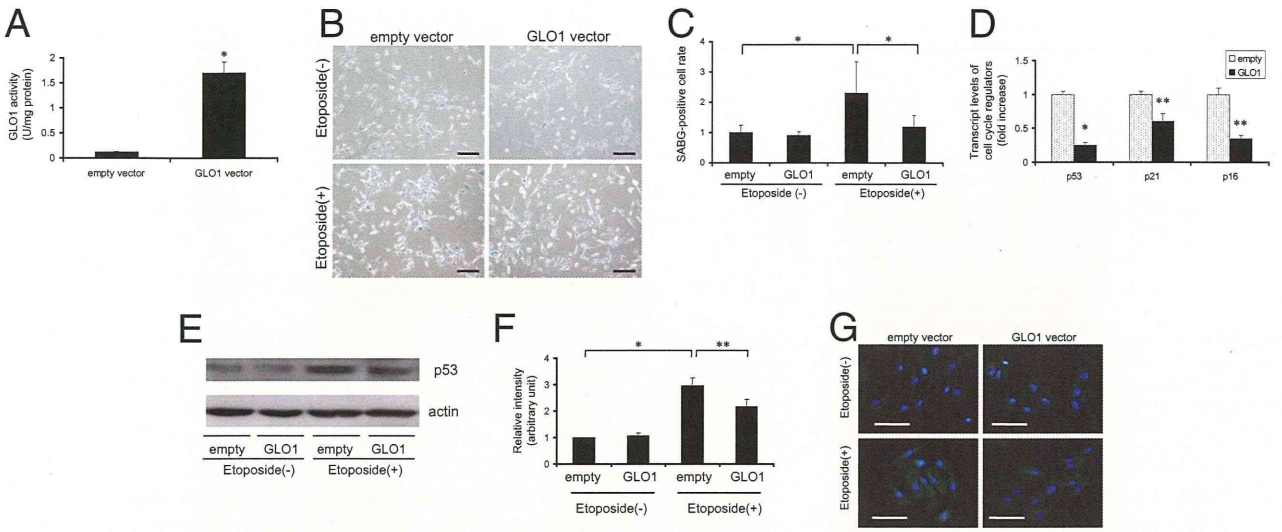

Figure 6. Attenuation of the senescent phenotypes of RPTECs at early passage with etoposide exposure by overexpression of GLO1. **A:** GLO1 activity assay measured at 24 hours after transfection of each vector confirmed successful overexpression of the transgene. Cells were lysed with sodium phosphate buffer with 1% Triton X-100 surfactant. $*P < 0.01$ versus empty vector. **B:** Phase-contrast light micrographs with SABG staining of RPTECs at passages 3 to 4 transfected with empty vector or GLO1-containing vector with or without etoposide exposure showed amelioration of senescence by GLO1. Original magnification = ×100. Scale bars: 200 μm. Blue stain indicates SABG-positive cells. **C:** Quantitative analysis of SABG-positive cells per total cells in each field. $*P < 0.01$ versus cells without etoposide exposure and transfected with empty vector. **D:** Relative transcript levels of p53, $p21^{WAF1/CIP1}$, and $p16^{INK4A}$ of RPTECs with etoposide exposure and transfected with plasmid vector determined by real-time quantitative RT-PCR. All showed a significant decrease in GLO1 transfectants, which demonstrated that GLO1 protected RPTECs against cellular senescence. Values of those transfected with empty vector were set as 1. $*P < 0.01$; $**P < 0.05$ versus cells transfected with empty vector. **E:** Protein immunoblot of p53 of whole lysate of RPTECs with or without etoposide exposure and transfected with plasmid vectors. p53 level in cells treated with etoposide exposure was ameliorated by GLO1 introduction. Actin serves as a control. **F:** Densitometric quantification of p53 immunoblot of RPTECs with or without etoposide exposure and transfected with plasmid vectors. The level of those transfected with empty vector without etoposide exposure was set as 1. $*P < 0.01$; $**P < 0.05$ versus cells without etoposide exposure and transfected with empty vector. **G:** Immunofluorescent micrographs of RPTECs with or without etoposide exposure and transfected with plasmid vectors for the detection of CEL accumulation. Cytosolic positive signals in cells exposed to etoposide were decreased by GLO1 introduction, demonstrating that overexpression of GLO1 ameliorated carbonyl stress. Green indicates anti-CEL (fluorescein isothiocyanate); blue stain identifies nuclei (Hoechst 33258 dye). Original magnification = ×400. Scale bars: 100 μm.

We also performed loss-of-function experiments with siRNA targeted to human GLO1 using two independent siRNAs against GLO1, which efficiently knocked down GLO1 expression and activity (Figure 7, A and B). Of note, when GLO1-knocked down cells were treated with etoposide, the number of cells positive for SABG staining was significantly increased, compared with control siRNA-transfected cells (Figure 7, C and D). Other senescence markers, such as transcript expression level of p53, $p21^{WAF1/CIP1}$, and $p16^{INK4A}$ or protein expression level of p53 in whole cellular lysate, were also markedly augmented by knockdown of GLO1 (Figure 7, E–G).

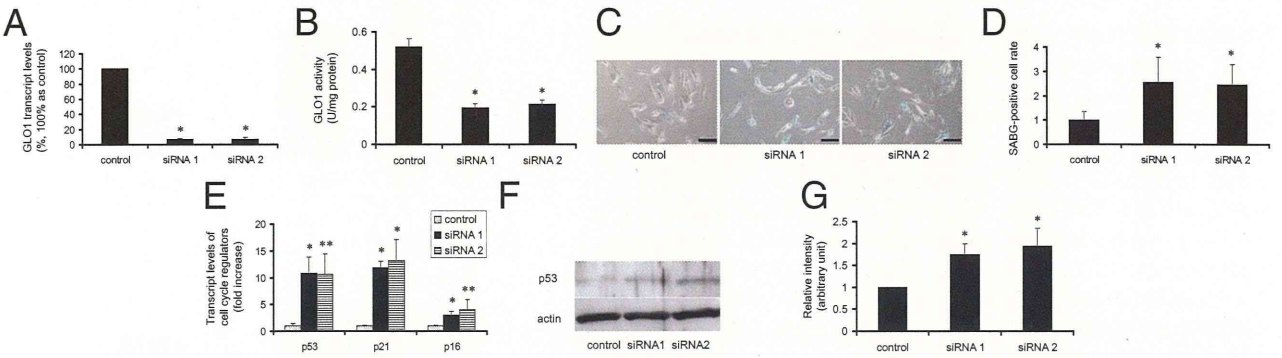

Figure 7. Knockdown of GLO1 exacerbated the senescence phenotype of RPTECs at early passage with etoposide exposure. **A:** Knockdown of the target gene was confirmed by transcript levels of GLO1 determined by real-time quantitative RT-PCR after 24 hours of transfection. The level of RPTECs transfected with control siRNA was set as 1. $*P < 0.01$ versus control siRNA. **B:** GLO1 activity assay measured after 24 hours transfection with siRNA or control RNA was consistent with the decreased transcript levels. $*P < 0.01$ versus empty vector. **C:** Phase-contrast light micrographs with SABG staining of RPTECs transfected with siRNA or control RNA with etoposide exposure showed aggravation of senescence by knockdown of GLO1. Original magnification = ×100. Scale bars: 100 μm. Blue stain indicates SABG-positive cells. **D:** Quantitative analysis of SABG-positive cells per total cells in each field. $*P < 0.05$ versus cells with etoposide exposure and transfected with control siRNA. **E:** Relative transcript levels of p53, $p21^{WAF1/CIP1}$, and $p16^{INK4A}$ of RPTECs with etoposide exposure and transfected with siRNA or control RNA determined by real-time quantitative RT-PCR showed that knockdown of GLO1 aggravated cellular senescence phenotypes. Values of those transfected with control siRNA were set as 1. $*P < 0.01$; $**P < 0.05$ versus cells with etoposide exposure and transfected with control siRNA. **F:** Protein immunoblot of p53 of whole lysate of RPTECs with etoposide exposure and transfected with siRNA or control RNA. The level of p53 from cells exposed to etoposide was aggravated by the knockdown of GLO1. Actin serves as a control. **G:** Densitometric quantification of p53 immunoblot. The level of cells transfected with control siRNA was set as 1. $*P < 0.05$ versus cells transfected with control siRNA.

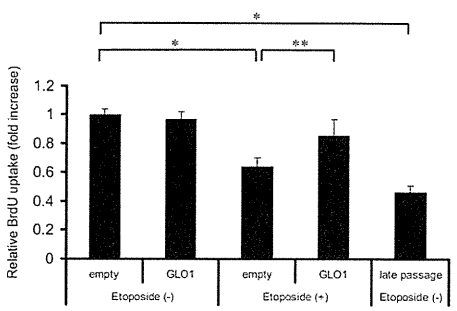

Figure 8. The replicative senescence induced by etoposide exposure was attenuated by transfection with the GLO1-overexpressing vector. BrdU uptake of RPTECs at early passage with or without etoposide exposure and at late passage without etoposide exposure was measured. BrdU uptake was significantly decreased by the addition of etoposide or at late passage, whereas the introduction of GLO1 ameliorated this decrease significantly. The level after transfection with empty vector without etoposide exposure was set as 1. $^{*}P < 0.01$; $^{**}P < 0.05$.

These gain-of-function and loss-of-function studies of GLO1 in cultured cells suggest that GLO1 has a cytoprotective effect against senescence.

Next, we verified the phenomena observed in the study of premature senescence by examining the status of replicative senescence on treatment with etoposide. Etoposide induced a significantly lower uptake of BrdU in RPTECs with mock transfection, and the degree of inhibition of BrdU uptake by etoposide was equivalent to that of late-passaged RPTECs (Figure 8). In contrast, cells overexpressing GLO1 showed no significant etoposide-induced decrease in the uptake of BrdU. These data demonstrate that the senescence status induced by etoposide, in which growth was inhibited and senescence markers were up-regulated, was ameliorated by GLO1.

Confirmation of Decrease in Renal Function of the Elderly Human Subjects with GLO1 Mutation

We had previously performed a nationwide analysis of GLO1 genotypes in schizophrenia patients and found that a minor subset of patients had frameshift mutations in GLO1.[24] Severe and significant decrease in the enzymatic activity was observed in those with frameshift mutations (3.0 ± 0.2 mU/10^6 red blood cells; n = 3), compared with WT GLO1 (6.8 ± 0.9 mU/10^6 red blood cells; n = 244). We investigated the effect of GLO1 activity on renal function. In the very rare cases with frameshift mutations, patients were all at the age of 50 to 60 years. We therefore compared the patients at this age, because GFR decreases with age.

Age-matched patients with WT GLO1 (n = 15) and frameshift mutation (n = 3) were analyzed. No clinically significant hematuria or proteinuria was found in any of the patients, with or without mutation. Neither musculature (determined by body mass index) nor systolic blood pressure, which could affect the serum creatinine levels, were significantly different among the three groups (Table 2). None of the patients with or without frameshift mutations were being treated with medication

Table 2. Physiological Characteristics of Elderly Schizophrenia Patients with or without *GLO1* Mutation

Characteristics	*GLO1* genotype	
	WT (n = 15)	Frameshift (n = 3)
Age (years)	56 ± 2.7	57 ± 4.6
Body mass index	23 ± 2.5	23 ± 4.9
Systolic blood pressure (mmHg)	110 ± 14	110 ± 11

No significant differences were observed in mean age, body mass index, or systolic blood pressure.

that could deteriorate renal functions. We reconfirmed a decreased activity of GLO1 in the patients with frameshift mutation, compared with the wild type (Figure 9A). Analysis of eGFR of the aged schizophrenia patients who had GLO1 frameshift mutations revealed significantly decreased renal function, compared with the wild type ($P <$ 0.01) (Figure 9B). The data confirmed the protective effect of GLO1 against an age-dependent decrease in renal function.

Discussion

We found that the aged kidney shows an increase in AGE accumulation in association with a decrease in GLO1 activity, as is seen also in the aged human lens,[26] aged human red blood cells,[21] and aged human brain.[27,28] Thus, age-dependent acceleration of carbonyl stress may induce renal senescence, at least in part. Accordingly, GLO1 might reduce the senescence phenotype via inhibitory activity against carbonyl stress.[9] In the present study, we have demonstrated for the first time both *in vitro*

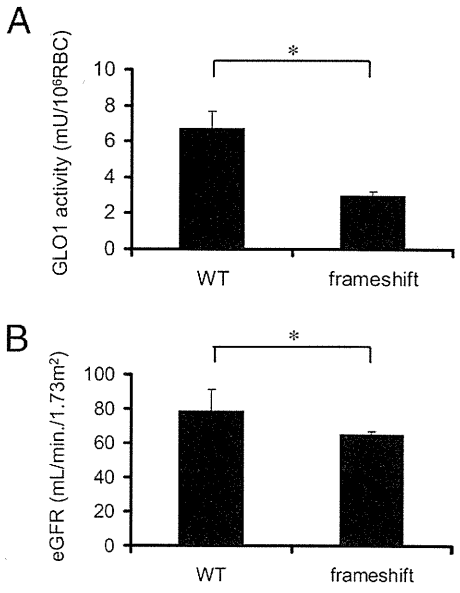

Figure 9. Analysis of human subjects with or without GLO mutations. **A:** GLO1 activity of red blood cells between the age-matched subjects with WT GLO1 and those with frameshift mutations of GLO1. WT, n = 15; frameshift, n = 3. $^{*}P < 0.01$. **B:** eGFR between age-matched subjects with WT GLO1 and those with frameshift mutations of GLO1. WT, n = 15; frameshift, n = 3. $^{*}P < 0.01$.

and *in vivo* that overexpression of GLO1 ameliorates all phenotypes of renal senescence. The delay in renal senescence in rats overexpressing GLO1 was associated with the preservation of kidney function. Furthermore, knockdown of GLO1 aggravated senescent phenotypes *in vitro*. Supporting a protective role of GLO1 against senescence, a recent report showed that overexpression of the GLO1 homolog CeGly induced longevity in *Caenorhabditis elegans*.[29]

We used 14-month-old rats for the aged group because we observed obvious histological changes associated with senescence in kidney in our preliminary experiments, as reported previously.[30] Because the aging process is complex and is likely to involve various mechanisms at different ages, we decided to focus on early senescence.

We focused our studies of kidney senescence on tubular epithelial cells. Functional impairment of the kidney more closely correlates with the degree of tubulointerstitial damage than with that of glomerular injury, and age-related decrease of eGFR is reported to be independent of glomerular change.[31] Our approach is consistent with several recent studies that have focused on tubulointerstitial alterations in the aging kidney.[30,32,33] One reason for the propensity toward senescence in the tubulointerstitium may relate to the metabolic rates of cells, given that podocytes or endothelial cells have far fewer mitochondria than tubular epithelial cells.[34]

In examination of a human specimen obtained from renal biopsy, we identified interstitial thickening (characterized by augmentation of matrix between tubules) as one of the senescent phenotypes of kidney. This alteration of renal components is distinct from interstitial fibrosis. Interstitial fibrosis is characterized by the replacement of tubules to fibrotic components and is observed in only limited portions of kidney, whereas interstitial thickening is a generalized change in the kidney. More importantly, this age-related phenotype is observed across a wide range of ages; in contrast, thickness of glomerular basement membrane is reported to have different effects at different ages.[35] To prevent overestimation of the interstitial thickness for tubules at an angle to the cutting surface, we measured the smallest thickness around tubules.

In the present study, RPTECs reached replicative senescence status at 10 passages, which is earlier than for primary cultured fibroblasts, which do so at approximately 40 passages. This finding is consistent with a previous report,[36] and might reflect high metabolic rate, susceptibility to senescence, or the nature of high differentiation. We also used etoposide, a well-established chemical senescence inducer,[37–40] to induce the cultured cells into senescence. The senescent phenotypes induced by etoposide were equivalent to those observed in late-passaged cells (although we note that the mechanism by which etoposide induces senescence has not been clarified).

The expression of senescence markers such as SABG, $p16^{INK4A}$, $p21^{WAF1/CIP1}$, and p53 was significantly increased in both late-passaged primary tubular epithelial cells and in the tubules of aged rat kidneys. Staining for p53 was positive not only in the nuclei but also in the cytoplasm, as reported previously.[41,42] These senescent phenotypes were associated *in vivo* with interstitial thickening in both human and rat kidney. Interstitial thickening might represent an aging-specific morphological change at an early stage of kidney aging. Similar changes were observed in a rodent model that was enhanced to present an age-related phenotype.[43,44]

Our analysis of schizophrenia patients demonstrated association of reduction of GLO1 activity and accelerated age-dependent deterioration of renal function in human. Age-dependent decline of renal function in subjects with preserved GLO1 activity was consistent with that described in healthy aged individuals previously (0.64 to 0.75 mL/min per year).[45–47] These results suggest that the difference in deterioration of age-dependent renal function that we observed was not due to improvement of renal function in schizophrenia patients with preserved GLO1 activity but rather was due to acceleration of age-dependent renal dysfunction associated with decreased GLO1 activity. One limitation is that these data are based on a small number of subjects in the GLO1-mutated group ($n = 3$); however, the incidence rate of this mutation is so low that this difficulty cannot be avoided.

Although excessive carbonyl stress is considered to be a major cause of spontaneous damage to intracellular and extracellular proteins functions,[48] detailed mechanisms of the progression of senescence by carbonyl stress remain to be elucidated.

In conclusion, we have established a role of carbonyl stress in senescence and demonstrated that GLO1 can retard renal senescence both *in vitro* and *in vivo*.

References

1. Dimri GP, Lee X, Basile G, Acosta M, Scott G, Roskelley C, Medrano EE, Linskens M, Rubelj I, Pereira-Smith O, Peacocke M, Campisi J: A biomarker that identifies senescent human cells in culture and in aging skin in vivo. Proc Natl Acad Sci USA 1995, 92:9363–9367
2. Duncan EL, Wadhwa R, Kaul SC: Senescence and immortalization of human cells. Biogerontology 2000, 1:103–121
3. Collado M, Serrano M: The power and the promise of oncogene-induced senescence markers. Nat Rev Cancer 2006, 6:472–476
4. Harman D: Aging: a theory based on free radical and radiation chemistry. J Gerontol 1956, 11:298–300
5. Perez VI, Bokov A, Remmen HV, Mele J, Ran Q, Ikeno Y, Richardson A: Is the oxidative stress theory of aging dead? Biochim Biophys Acta 2009, 1790:1005–1014
6. Pérez VI, Van Remmen H, Bokov A, Epstein CJ, Vijg J, Richardson A: The overexpression of major antioxidant enzymes does not extend the lifespan of mice. Aging Cell 2009, 8:73–75
7. Stadtman ER: Protein oxidation and aging. Science 1992, 257:1220–1224
8. Thorpe SR, Baynes JW: Role of the Maillard reaction in diabetes mellitus and diseases of aging. Drugs Aging 1996, 9:69–77
9. Thornalley PJ: Protein and nucleotide damage by glyoxal and methylglyoxal in physiological systems: role in ageing and disease. Drug Metabol Drug Interact 2008, 23:125–150
10. Finkel T, Holbrook NJ: Oxidants, oxidative stress and the biology of ageing. Nature 2000, 408:239–247
11. Uribarri J, Cai W, Peppa M, Goodman S, Ferrucci L, Striker G, Vlassara H: Circulating glycotoxins and dietary advanced glycation endproducts: two links to inflammatory response, oxidative stress, and aging. J Gerontol A Biol Sci Med Sci 2007, 62:427–433
12. Münch G, Shepherd CE, McCann H, Brooks WS, Kwok JB, Arendt T, Hallupp M, Schofield PR, Martins RN, Halliday GM: Intraneuronal

advanced glycation endproducts in presenilin-1 Alzheimer's disease. Neuroreport 2002, 13:601–604
13. Ahmed N: Advanced glycation endproducts–role in pathology of diabetic complications. Diabetes Res Clin Pract 2005, 67:3–21
14. Chen J, Huang X, Halicka D, Brodsky S, Avram A, Eskander J, Bloomgarden NA, Darzynkiewicz Z, Goligorsky MS: Contribution of p16INK4a and p21CIP1 pathways to induction of premature senescence of human endothelial cells: permissive role of p53. Am J Physiol Heart Circ Physiol 2006, 290:H1575–H1586
15. Thangarajah H, Yao D, Chang EI, Shi Y, Jazayeri L, Vial IN, Galiano RD, Du XL, Grogan R, Galvez MG, Januszyk M, Brownlee M, Gurtner GC: The molecular basis for impaired hypoxia-induced VEGF expression in diabetic tissues. Proc Natl Acad Sci USA 2009, 106:13505–13510
16. Thornalley PJ: The glyoxalase system: new developments towards functional characterization of a metabolic pathway fundamental to biological life. Biochem J 1990, 269:1–11
17. Hayes JD, Milner SW, Walker SW: Expression of glyoxalase, glutathione peroxidase and glutathione S-transferase isoenzymes in different bovine tissues. Biochim Biophys Acta 1989, 994:21–29
18. Thornalley PJ: Glyoxalase I–structure, function and a critical role in the enzymatic defence against glycation. Biochem Soc Trans 2003, 31:1343–1348
19. Kumagai T, Nangaku M, Kojima I, Nagai R, Ingelfinger JR, Miyata T, Fujita T, Inagi R: Glyoxalase I overexpression ameliorates renal ischemia-reperfusion injury in rats. Am J Physiol Renal Physiol 2009, 296:F912–F921
20. Inagi R, Miyata T, Ueda Y, Yoshino A, Nangaku M, van Ypersele de Strihou C, Kurokawa K: Efficient in vitro lowering of carbonyl stress by the glyoxalase system in conventional glucose peritoneal dialysis fluid. Kidney Int 2002, 62:679–687
21. McLellan AC, Thornalley PJ: Glyoxalase activity in human red blood cells fractioned by age. Mech Ageing Dev 1989, 48:63–71
22. Nagai R, Fujiwara Y, Mera K, Yamagata K, Sakashita N, Takeya M: Immunochemical detection of Nepsilon-(carboxyethyl)lysine using a specific antibody. J Immunol Methods 2008, 332:112–120
23. Rutenburg AM, Kim H, Fischbein JW, Hanker JS, Wasserkrug HL, Seligman AM: Histochemical and ultrastructural demonstration of gamma-glutamyl transpeptidase activity. J Histochem Cytochem 1969, 17:517–526
24. Arai M, Yuzawa H, Nohara I, Ohnishi T, Obata N, Iwayama Y, Haga S, Toyota T, Ujike H, Arai M, Ichikawa T, Nishida A, Tanaka Y, Furukawa A, Aikawa Y, Kuroda O, Niizato K, Izawa R, Nakamura K, Mori N, Matsuzawa D, Hashimoto K, Iyo M, Sora I, Matsushita M, Okazaki Y, Yoshikawa T, Miyata T, Itokawa M: Enhanced carbonyl stress in a subpopulation of schizophrenia. Arch Gen Psychiatry 2010, 67:589–597
25. Matsuo S, Imai E, Horio M, Yasuda Y, Tomita K, Nitta K, Yamagata K, Tomino Y, Yokoyama H, Hishida A; Collaborators developing the Japanese equation for estimated GFR: Revised equations for estimated GFR from serum creatinine in Japan. Am J Kidney Dis 2009, 53:982–992
26. Haik GM Jr, Lo TW, Thornalley PJ: Methylglyoxal concentration and glyoxalase activities in the human lens. Exp Eye Res 1994, 59:497–500
27. Kuhla B, Boeck K, Lüth HJ, Schmidt A, Weigle B, Schmitz M, Ogunlade V, Münch G, Arendt T: Age-dependent changes of glyoxalase I expression in human brain. Neurobiol Aging 2006, 27:815–822
28. Kuhla B, Boeck K, Schmidt A, Ogunlade V, Arendt T, Münch G, Lüth HJ: Age- and stage-dependent glyoxalase I expression and its activity in normal and Alzheimer's disease brains. Neurobiol Aging 2007, 28:29–41
29. Morcos M, Du X, Pfisterer F, Hutter H, Sayed AA, Thornalley P, Ahmed N, Baynes J, Thorpe S, Kukudov G, Schlotterer A, Bozorgmehr F, El Baki RA, Stern D, Moehrlen F, Ibrahim Y, Oikonomou D, Hamann A, Becker C, Zeier M, Schwenger V, Miftari N, Humpert P, Hammes HP, Buechler M, Bierhaus A, Brownlee M, Nawroth PP: Glyoxalase-1 prevents mitochondrial protein modification and enhances lifespan in Caenorhabditis elegans. Aging Cell 2008, 7:260–269
30. Ding G, Franki N, Kapasi AA, Reddy K, Gibbons N, Singhal PC: Tubular cell senescence and expression of TGF-beta1 and p21(WAF1/CIP1) in tubulointerstitial fibrosis of aging rats. Exp Mol Pathol 2001, 70:43–53
31. Rule AD, Am H, Cornell LD, Taler SJ, Cosio FG, Kremers WK, Textor SC, Stegall MD: The association between age and nephrosclerosis on renal biopsy among healthy adults. Ann Intern Med 2010, 152:561–567
32. Abrass CK, Adcox MJ, Raugi GJ: Aging-associated changes in renal extracellular matrix. Am J Pathol 1995, 146:742–752
33. Ruiz-Torres MP, Bosch RJ, O'Valle F, Del Moral RG, Ramírez C, Masseroli M, Pérez-Caballero C, Iglesias MC, Rodríguez-Puyol M, Rodríguez-Puyol D: Age-related increase in expression of TGF-beta1 in the rat kidney: relationship to morphologic changes. J Am Soc Nephrol 1998, 9:782–791
34. Pease DC: Fine structures of the kidney seen by electron microscopy. J Histochem Cytochem 1955, 3:295–308
35. Shindo S, Yoshimoto M, Kuriya N, Bernstein J: Glomerular basement membrane thickness in recurrent and persistent hematuria and nephrotic syndrome: correlation with sex and age. Pediatr Nephrol 1988, 2:196–199
36. Glynne PA: Primary culture of human proximal renal tubular epithelial cells. Methods Mol Med 2000, 36:197–205
37. Krizhanovsky V, Yon M, Dickins RA, Hearn S, Simon J, Miething C, Yee H, Zender L, Lowe SW: Senescence of activated stellate cells limits liver fibrosis. Cell 2008, 134:657–667
38. te Poele RH, Okorokov AL, Jardine L, Cummings J, Joel SP: DNA damage is able to induce senescence in tumor cells in vitro and in vivo. Cancer Res 2002, 62:1876–1883
39. Robles SJ, Buehler PW, Negrusz A, Adami GR: Permanent cell cycle arrest in asynchronously proliferating normal human fibroblasts treated with doxorubicin or etoposide but not camptothecin. Biochem Pharmacol 1999, 58:675–685
40. Wang Y, Blandino G, Oren M, Givol D: Induced p53 expression in lung cancer cell line promotes cell senescence and differentially modifies the cytotoxicity of anti-cancer drugs. Oncogene 1998, 17:1923–1930
41. Kaserer K, Schmaus J, Bethge U, Migschitz B, Fasching S, Walch A, Herbst F, Teleky B, Wrba F: Staining patterns of p53 immunohistochemistry and their biological significance in colorectal cancer. J Pathol 2000, 190:450–456
42. Ranade KJ, Nerurkar AV, Phulpagar MD, Shirsat NV: Expression of survivin and p53 proteins and their correlation with hormone receptor status in Indian breast cancer patients. Indian J Med Sci 2009, 63:481–490
43. Samuel CS, Zhao C, Bond CP, Hewitson TD, Amento EP, Summers RJ: Relaxin-1-deficient mice develop an age-related progression of renal fibrosis. Kidney Int 2004, 65:2054–2064
44. Floege J, Hackmann B, Kliem V, Kriz W, Alpers CE, Johnson RJ, Kühn KW, Koch KM, Brunkhorst R: Age-related glomerulosclerosis and interstitial fibrosis in Milan normotensive rats: a podocyte disease. Kidney Int 1997, 51:230–243
45. Lindeman RD, Tobin J, Shock NW: Longitudinal studies on the rate of decline in renal function with age. J Am Geriatr Soc 1985, 33:278–285
46. Rowe JW, Andres R, Tobin JD: Letter: age-adjusted standards for creatinine clearance. Ann Intern Med 1976, 84:567–569
47. Rowe JW, Andres R, Tobin JD, Norris AH, Shock NW: The effect of age on creatinine clearance in men: a cross-sectional and longitudinal study. J Gerontol 1976, 31:155–163
48. Thornalley PJ, Battah S, Ahmed N, Karachalias N, Agalou S, Babaei-Jadidi R, Dawnay A: Quantitative screening of advanced glycation endproducts in cellular and extracellular proteins by tandem mass spectrometry. Biochem J 2003, 375:581–592

of the Wechsler Intelligence Scale, third edition (WAIS-III), his full-scale intelligence quotient (IQ) was 124, verbal IQ was 130, and performance IQ was 112. Marked deviations were seen in some subtests of the WAIS-III, with very high performance in Vocabulary and Information, and very low performance in Letter–number sequencing and Picture completion. Magnetic resonance imaging (MRI) of the head and encephalography yielded results within normal limits. These findings suggested autistic disorder (high-functioning autism) according to DSM-IV-TR criteria.

Collagens represent a large family of structurally related extracellular matrix proteins essential for development, cell attachment, platelet aggregation and tensile strength in connective tissues such as bone, skin, ligaments, tendons, and blood vessels.[3] Cupo *et al.* described abnormalities in the development of the central nervous system (CNS) in EDS, including a heterotropic formation in the CNS.[4] Although no CNS abnormality was evident on MRI in the present case, loss of elasticity and strength of collagen presumably contributed to structural failure in connective tissues of the CNS. We speculate that associations exist between connective tissue diseases and autistic disorders, and that connective tissue abnormalities may contribute to autistic symptoms.

REFERENCES

1. Tantam D, Evered C, Hersov L. Asperger's syndrome and ligamentous laxity. *J. Am. Acad. Child Adolesc. Psychiatry* 1990; 29: 892–896.
2. Sieg KG. Autism and Ehlers-Danlos syndrome. *J. Am. Acad. Child Adolesc. Psychiatry* 1992; 31: 173.
3. De Paepe A, Malfait F. Bleeding and bruising in patients with Ehlers-Danlos syndrome and other collagen vascular disorders. *Br. J. Haematol.* 2004; 127: 491–500.
4. Cupo LN, Pyeretz R, Olson J, McPhee S, Hutchins G, McKusick V. Ehlers-Danlos syndrome with abnormal collagen fibrils, sinus of Valsalva aneurysms, myocardial infraction, panacinar emphysema and cerebral heterotopics. *Am. J. Med.* 1981; 71: 1051–1058.

Akira Takei, MD, Kazuhiko Mera, MD, Yuzuru Sato, MD and Yoichi Haraoka, MD

Department of Psychiatry, Asahikawa City Hospital, Asahikawa, Japan

Email: a_takei@city.asahikawa.hokkaido.jp

Received 20 April 2011; revised 21 June 2011; accepted 8 August 2011.

Idiopathic carbonyl stress in a drug-naive case of at-risk mental state

doi:10.1111/j.1440-1819.2011.02261.x

WE PREVIOUSLY REPORTED that a subgroup of schizophrenia patients exhibit carbonyl stress with high plasma pentosidine levels, without underlying diabetes mellitus or chronic kidney disease, the two major causes of elevated, advanced glycation end-products.[1] These patients, however, had previously received antipsychotic therapy, leaving the possible role of medication in carbonyl stress unclear. Here, we report on a drug-naive patient with at-risk mental state (ARMS), who exhibited enhanced carbonyl stress with high plasma pentosidine levels.

The patient was a 21-year-old male college student, who was born at full term after an uneventful pregnancy and delivery. He first developed obsessive thoughts at age 18 and sought medical help because of communication difficulties and depression. He was diagnosed with obsessive and compulsive disorder (OCD) according to DSM-IV criteria. Biweekly counseling and psychotherapy temporarily reduced his symptoms but a persistence of confused thoughts, hearing hypersensitivity and delusional ideation of persecution and reference led to a diagnosis of ARMS, according to Structured Interview for Prodromal Syndromes (SIPS) criteria, 10 months after his initial consultation. He was followed clinically for 12 months and treated temporarily with 0.5 mg of etizolam and 5 mg of zolpidem, which improved his symptoms. He entered a research study on ARMS and his symptoms were scaled and biochemical data measured at his initial visit, and also after 16 months of treatment. During this period his score on the Positive and Negative Syndrome Scale decreased from 84 to 58 ($P = 0.001$), his positive subscale score changed from 20 to 22 ($P = 0.38$), negative subscale score changed from 22 to 9 ($P = 0.03$) and the general psychopathology subscale score changed from 42 to 27 ($P = 0.008$). Global Assessment of Functioning also improved from 55 to 65. Plasma pentosidine levels decreased from 113.2 to 44.1 ng/mL. We did not measure carbonyl compounds such as methylglyoxal (MG), carbohydrate precursors of pentosidine and advanced glycation adducts: *N*(ε)-(carboxymethyl)lysine and *N*(ε)-(carboxyethyl)lysine. We did not assess the activity of glyoxalase1 (GLO1) or pyridoxal levels before treatment, but after treatment the activity was 7.55 mU/10^6 red blood cells, and the pyridoxal level was 6.8 ng/mL, and these are both normal levels for the enzyme and pyridoxal, respectively. It is not known whether etizolam and zolpidem affect pentosidine levels. In the preliminary data, the dose (mg/day) of etizolam ($n = 18$) or zolpidem ($n = 11$) was not significantly correlated with pentosidine levels in patients with schizophrenia (data not shown). The patients were also taking other drugs, however, and thus the lack of apparent correlation is not conclusive. The GLO1 genotype in the present case was wild type (c.332A>C, p.Glu111/Glu111). Biochemistry did not demonstrate any abnormalities indicative of disease, such as diabetes mellitus or chronic kidney diseases.

The present case report does not demonstrate a direct link between carbonyl stress and the disease development. It is not known whether carbonyl stress is a cause or consequence of the disease. In addition, it cannot be ruled out that other physical conditions or drugs affected the pentosidine levels. Additional data are needed to clarify a possible relationship between carbonyl stress and mental disorders.

The ethics committees for the University of Tokyo and Tokyo Institute of Medical Science approved the present study (2089-(2), 2094-(2), 2226-(1), 21–2). The subject gave written informed consent in accordance with the Declaration of Helsinki after a complete explanation of the original study. After

ethics approval, the patient re-consented for publication of this case report.

This study was supported by grants from the Ministry of Health, Labour, and Welfare (H22-seishin-ippan-015 to KK), and from the JSPS/MEXT (No. 21249064 and Grant-in-Aid for Scientific Research on Innovative Areas [Comprehensive Brain Science Network] to KK, No. 20249054 and Grant-in-Aid for Scientific Research (A), no. 22129007 and Grant-in-Aid for Scientific Research on Priority Areas to MI). A part of this study was also the result of 'Development of biomarker candidates for social behavior' carried out under the Strategic Research Program for Brain Sciences by MEXT.

REFERENCE

1. Arai M, Yuzawa H, Nohara I *et al.* Enhanced carbonyl stress in a subpopulation of schizophrenia. *Arch. Gen. Psychiatry* 2010; 67: 589–597.

Makoto Arai, PhD,[1] Shinsuke Koike, MD,[2] Norihito Oshima, MD,[3] Ryu Takizawa, MD,[2] Tsuyoshi Araki, MD, PhD,[2] Mitsuhiro Miyashita, MD,[1] Atsushi Nishida, PhD,[1] Toshio Miyata, MD, PhD,[4] Kiyoto Kasai, MD, PhD[2] and Masanari Itokawa, MD, PhD[1]

[1]Project for Schizophrenia and Affective Disorders Research, Tokyo Metropolitan Institute of Medical Science, [2]Department of Neuropsychiatry, Graduate School of Medicine, [3]Division for Counseling and Support, Office for Mental Health Support, University of Tokyo, Tokyo, and [4]Center for Translational and Advanced Research on Human Disease, Tohoku University Graduate School of Medicine, Miyagi, Japan

Email: itokawa-ms@igakuken.or.jp

Received 27 April 2011; revised 7 July 2011; accepted 8 August 2011.

Aripiprazole monotherapy in the treatment of vascular parkinsonism

doi:10.1111/j.1440-1819.2011.02263.x

VASCULAR PARKINSONISM (VP) is characterized by poor response to levodopa. In contrast, reduced presynaptic dopaminergic activity, the main pathology of Parkinson's disease (PD), is not suggested in VP.[1] Dopamine D2 partial agonists have been suggested as a potential therapeutic approach to the treatment of the motor symptoms of PD that may avoid common dopaminergic side-effects including dyskinesia and psychosis.[2] We report a first case of antiparkinsonian agent-refractory VP in which both psychosis and parkinsonism were treated successfully using aripiprazole monotherapy.

A 75-year-old woman with an 8-year history of antiparkinsonian agent-refractory VP was admitted to Department of Neuropsychiatry, Fukui University Hospital for treatment for psychosis. On admission, treatment consisted of 400 mg/day of L-dopa/carbidopa, 100 mg/day of droxidopa, and 100 mg/day of amantadine. The patient had showed postural tremor, gait disorder, and pyramidal signs with lower-body predominance and mild cognitive impairment (Mini-Mental State Examination: 22/30). The severity score on the Unified Parkinson's Disease Rating Scale (UPDRS) was 118. The illness stage according to the Hoehn and Yahr scale was IV. The patient exhibited frank psychosis with vivid visual hallucinations and fearful delusions of persecution (severity score on the Brief Psychiatric Rating Scale [BPRS] was 96). Results of laboratory tests, electrocardiography, and electroencephalography were normal. Myocardial ^{123}I-metaiodobenzylguanidine indicated a normal heart to mediastinum ratio; cranial magnetic resonance imaging showed multiple deep subcortical lesions. Antiparkinsonian medications were gradually tapered off with no apparent clinical changes of parkinsonism. Her psychotic symptoms improved to a large extent (BPRS score, 52) on day 20, but visual hallucinations persisted. On day 34, aripiprazole monotherapy was started at 3 mg/day and increased by 3 mg every week up to 9 mg. Her psychosis gradually improved (BPRS score, 32), with dramatic amelioration of parkinsonism (UPDRS score, 43), especially in activities of daily living and motor examination items of UPDRS. Using the same regimen, no worsening of psychiatric or neurological symptoms had occurred 7 months after discharge.

In the present case, aripiprazole improved pharmacologically paradoxical symptoms such as psychosis and parkinsonism by the stabilization of dopaminergic activity through dopamine D2 partial agonistic properties.[3] Cerebrovascular lesions, which are suggested as a mechanism for VP,[1] might cause not reduced presynaptic dopaminergic activity but dysregulated dopaminergic activity. Although the utility of aripiprazole in managing psychosis and parkinsonism in PD remains controversial,[4,5] the present case suggests the potential utility of aripiprazole monotherapy in treating VP.

REFERENCES

1. Kalra S, Grosset DG, Benamer HT. Differentiating vascular parkinsonism from idiopathic Parkinson's disease: A systematic review. *Mov. Disord.* 2010; 25: 149–156.
2. Bronzova J, Sampaio C, Hauser RA *et al.* Double-blind study of pardoprunox, a new partial dopamine agonist, in early Parkinson's disease. *Mov. Disord.* 2010; 25: 730–738.
3. Jordan S, Koprivica V, Dunn R, Tottori K, Kikuchi T, Altar CA. In vivo effects of aripiprazole on cortical and striatal dopaminergic and serotonergic function. *Eur. J. Pharmacol.* 2004; 483: 45–53.
4. Fernandez HH, Trieschmann ME, Friedman JH. Aripiprazole for drug-induced psychosis in Parkinson disease: Preliminary experience. *Clin. Neuropharmacol.* 2004; 27: 4–5.
5. Fujino J, Tanaka H, Taniguchi N, Tabushi K. Effectiveness of aripiprazole in a patient with presumed idiopathic Parkinson's disease and chronic paranoid schizophrenia. *Psychiatry Clin. Neurosci.* 2010; 64: 108–109.

Makoto Ishitobi, MD, PhD, Hirotaka Kosaka, MD, PhD, Tetsuya Takahashi, MD, PhD, Makiyo Oonuma, MD, Tetsuhito Murata, MD, PhD and Yuji Wada, MD, PhD

Department of Neuropsychiatry, University of Fukui, Fukui, Japan

Email: mak1977019@yahoo.co.jp

Received 21 June 2011; revised 29 July 2011; accepted 8 August 2011.

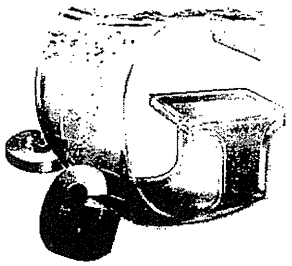

精神科救急における高齢者
―― 措置入院の運用と患者の臨床特性 ――

湯本洋介，新里和弘，斎藤正彦

抄　録

本論においては近年の措置入院患者数，とくに高齢者の動向，ならびに東京都立松沢病院における高齢救急患者の臨床特性について考察を行った．措置入院全体に占める高齢者の割合が漸増傾向にあることが示され，精神科救急の場で自傷他害の危険性の高い高齢者に遭遇する機会が今後増えることが予測された．高齢者には認知症や身体合併症など特有な病態があり，精神―身体の両面を含めた診断と治療のスキルがわれわれに求められる．また精神科救急で有意な増加を示す高齢統合失調症に関する考察も行った．

Key words：精神科救急，措置入院，高齢者，統合失調症

老年精神医学雑誌 23：1316-1322，2012

はじめに

わが国では他国に類をみない急激なスピードで高齢化が進んでいる．高齢者人口（65歳以上）は増加の一途をたどり，それに伴い高齢化率も増加し，2013年には国民の4人に1人が高齢者，2035年には3人に1人が，2060年には2.5人に1人が高齢者の時代が到来することが予想されている．高齢者人口の増加に伴い，高齢者を対象とした保健・医療・福祉制度の整備が進められている．

精神科救急も地域内における重要な精神保健サービスの一環である[10]．本論では，精神科救急のうち，自傷他害の可能性の高い患者を対象としたいわゆる「ハード救急」について考察を行う．筆者らの調査[11,12]によると，東京都の精神科救急（「ハード救急」）に搬送される高齢者の数は10年間で約1.6倍に増加していた．精神科救急における高齢患者の実態について把握検討を行うことは高齢者の精神障害に対する精神保健サービスのあり方を考えていくうえで欠かせない課題である．

措置入院は「精神保健及び精神障害者福祉に関する法律」の第29条で定められた入院形態である．その適応は「ただちに入院させなければ，精神障害のために自身を傷つけ，または他人を害するおそれがある」状態と規定されており，精神科ハード救急で頻用される入院形態である．高齢者でも著しい興奮状態などで精神科救急に搬送される患者はまれならずあるが，その詳細に関してはほとんど報告がなされていない．

本論では，その前半で高齢者の措置入院の動向を，全国および東京都の調査をもとに概観する．後半では東京都立松沢病院（以下，当院）における高齢精神科救急患者の臨床特性を抽出し考察を行い，今後の高齢者向け保健医療サービスを考えるうえでの一助としたい．

Yosuke Yumoto, Kazuhiro Niizato, Masahiko Saito：東京都立松沢病院
〒156-0057　東京都世田谷区上北沢2-1-1